

Pentagon contact representations*

Stefan Felsner[†] Hendrik Schrezenmaier[†] Raphael Steiner

Institut für Mathematik
Technische Universität Berlin
Germany

`{felsner,schrezen,steiner}@math.tu-berlin.de`

Aug 1, 2018

Abstract

Representations of planar triangulations as contact graphs of a set of internally disjoint homothetic triangles or of a set of internally disjoint homothetic squares have received quite some attention in recent years. In this paper we investigate representations of planar triangulations as contact graphs of a set of internally disjoint homothetic pentagons. Surprisingly such a representation exists for every triangulation whose outer face is a 5-gon. We relate these representations to *five color forests*. These combinatorial structures resemble Schnyder woods and transversal structures, respectively. In particular there is a bijection to certain α -orientations and consequently a lattice structure on the set of five color forests of a given graph. This lattice structure plays a role in an algorithm that is supposed to compute a contact representation with pentagons for a given graph. Based on a five color forest the algorithm builds a system of linear equations and solves it, if the solution is non-negative, it encodes distances between corners of a pentagon representation. In this case the representation is constructed and the algorithm terminates. Otherwise negative variables guide a change of the five color forest and the procedure is restarted with the new five color forest. Similar algorithms have been proposed for contact representations with homothetic triangles and with squares.

Mathematics Subject Classifications: 05C62, 68R10

1 Introduction

A *pentagon contact system* \mathcal{S} is a finite system of convex pentagons in the plane such that any two pentagons intersect in at most one point. If all pentagons of \mathcal{S} are regular

*This paper has appeared in the Electronic Journal of Combinatorics (E-JC 25.3 (2018), P3.39). The conference version of this paper has appeared in the proceedings of Eurocomb'17 (ENDM 61C, pp. 421–427) under the same title.

[†]Partially supported by DFG grant FE-340/11-1.

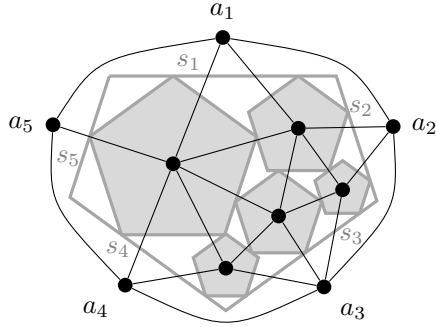


Figure 1: A regular pentagon contact representation of the graph shown in black.

pentagons with a horizontal side at the bottom, we call \mathcal{S} a *regular pentagon contact representation*. Note that in this case any two pentagons of \mathcal{S} are homothetic. The contact system is *non-degenerate* if every contact involves exactly one corner of a pentagon. The *contact graph* $\mathcal{G}(\mathcal{S})$ of \mathcal{S} is the graph that has a vertex for every pentagon and an edge for every contact of two pentagons in \mathcal{S} . Note that $\mathcal{G}(\mathcal{S})$ inherits a crossing-free embedding into the plane from \mathcal{S} . For a given plane graph G and a pentagon contact system \mathcal{S} with $\mathcal{G}(\mathcal{S}) = G$ we say that \mathcal{S} is a *pentagon contact representation* of G .

We will only consider the case that G is an *inner triangulation of a 5-gon*, i.e., the outer face of G is a 5-cycle with vertices a_1, \dots, a_5 in clockwise order, all inner faces are triangles, there are no loops nor multiple edges, and the only edges between the vertices a_1, \dots, a_5 are the five edges of the outer face. Our interest lies in a variant of regular pentagon contact representations of G with the property that a_1, \dots, a_5 are not represented by regular pentagons, but by line segments s_1, \dots, s_5 which together form a pentagon with all internal angles equal to $(3/5)\pi$. The line segment s_1 is always horizontal and at the top, and s_1, \dots, s_5 is the clockwise order of the segments of the pentagon. Since this variant of regular pentagon contact representations is the only kind of contact representations we deal with in this paper, we refer to these also as regular pentagon contact representations. Figure 1 shows an example.

Triangle contact representations have been introduced by de Fraysseix et al. [5]. They observed that Schnyder woods can be considered as combinatorial encodings of triangle contact representations of triangulations and essentially showed that any Schnyder wood can be used to construct a corresponding triangle contact system. They also showed that the triangles can be requested to be isosceles with a horizontal basis. Representations with homothetic triangles can degenerate in the presence of separating triangles. Gonçalves et al. [9] showed that 4-connected triangulations admit contact representations with homothetic triangles. The proof is an application of Schramm's *Convex Packing Theorem*, a strong theorem which is based on his *Monster Packing Theorem*. A more combinatorial approach to homothetic triangle contact representations which aims at computing the representation as the solution of a system of linear equations related to a Schnyder wood was described by Felsner [7]. On the basis of this approach Schrezenmaier proved the existence of homothetic triangle representations in his Master's thesis [18].

Representations of graphs using squares or more precisely graphs as a tool to model packings of squares already appear in classical work of Brooks et al. [3] from 1940. Schramm [17] proved that every 5-connected inner triangulation of a 4-gon admits a square contact representation. Again there is a combinatorial approach to this result which aims at computing the representation as the solution of a system of linear equations, see Felsner [8]. In this instance the role of Schnyder woods is taken by *transversal structures*. As in the case of homothetic triangles this approach comes with an algorithm which works well in practice, however, the proof that the algorithm terminates with a solution is still missing. On the basis of the non-algorithmic aspects of this approach Schrezenmaier [18] reproved Schramm’s Squaring Theorem.

In this paper we investigate representations of planar triangulations as contact graphs of a set of internally disjoint homothetic pentagons. From Schramm’s *Convex Packing Theorem* it easily follows that such a representation exists for every triangulation whose outer face is a 5-gon. We relate such representations to *five color forests*. The main part of the paper is devoted to the study of this combinatorial structure. It will become clear that five color forests are close relatives of Schnyder woods and transversal structures. We note in passing that Bernardi and Fusy [1] also studied some relatives of Schnyder woods using 5 colors. Their “five color trees”, however, only live on duals of 5-regular planar graphs.

At the end of the paper we propose an algorithm for computing homothetic pentagon representations on the basis of systems of equations and local changes in the corresponding five color forests. We conjecture that the algorithm always terminates. A proof of this conjecture would imply a proof for the existence of pentagon contact representations which is independent of Schramm’s Monster Packing. The idea of looking for pentagon contact representations and a substantial part of the work originate in the Bachelor’s Thesis of Steiner [19].

1.1 The existence of pentagon contact representations

The existence of regular pentagon contact representations for every inner triangulation of a 5-gon can be shown using the following general result about contact representations by Schramm.

Theorem 1 (Convex Packing Theorem [16]). *Let G be an inner triangulation of the triangle abc . Further let C be a simple closed curve in the plane partitioned into three arcs $\mathcal{P}_a, \mathcal{P}_b, \mathcal{P}_c$, and for each inner vertex v of G let \mathcal{P}_v be a convex set in the plane containing more than one point. Then there exists a contact representation of a supergraph of G (on the same vertex set, but possibly with more edges) where each inner vertex v is represented by a single point or a homothetic copy of its prototype \mathcal{P}_v and each outer vertex w by the arc \mathcal{P}_w .*

Theorem 2. *Let G be an inner triangulation of the 5-gon a_1, \dots, a_5 . Then there exists a regular pentagon contact representation of G .*

Proof. By adding the edges a_1a_3 and a_1a_4 in the outer face of G , it becomes a triangulation G' with outer face $a_1a_3a_4$. We define the arcs $\mathcal{P}_{a_1}, \mathcal{P}_{a_3}, \mathcal{P}_{a_4}$ to be extensions of the

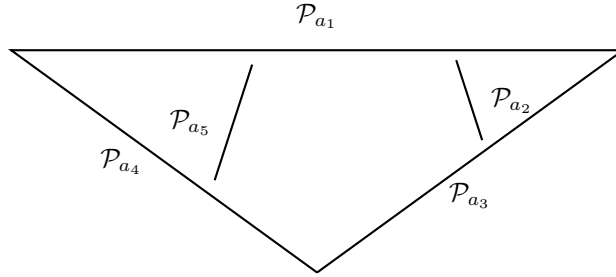


Figure 2: Prototypes for the five outer vertices of G .

upper, lower left and lower right edge of a regular pentagon A with a horizontal edge at the top, respectively, such that $\mathcal{P}_{a_1} \cup \mathcal{P}_{a_3} \cup \mathcal{P}_{a_4}$ forms a triangle and therefore a simple closed curve. We define the convex sets \mathcal{P}_{a_2} and \mathcal{P}_{a_5} to be line segments parallel to the upper right and upper left edge of the pentagon A (see Fig. 2). Finally, for each inner vertex v of G let \mathcal{P}_v be a regular pentagon with a horizontal edge at the bottom.

Now we can apply the Convex Packing Theorem. The result is a contact representation of a supergraph of G' where a_1, a_3, a_4 are represented by $\mathcal{P}_{a_1}, \mathcal{P}_{a_3}, \mathcal{P}_{a_4}$ and every inner vertex v by a homothetic copy of \mathcal{P}_v or by a single point.

We claim that in this contact representation of G' none of the homothetic copies of the prototypes is degenerate to a single point. Assume there is a degenerate copy in the contact representation. Let H be a maximal connected component of the subgraph of G' induced by the vertices whose pentagons are degenerate to a single point. Since the line segments corresponding to the three outer vertices are not degenerate, H has to be bounded by a cycle C of vertices whose pentagons or line segments are not degenerate. In the contact representation all vertices of H are represented by the same point and therefore all pentagons and line segments representing the vertices of C have a contact with this point, i.e., they meet at the point. But for geometric reasons at most two of these can meet in a single point. Thus C is a 2-cycle, in contradiction to our definition of inner triangulations that does not allow multiple edges.

After cutting the segments $\mathcal{P}_{a_1}, \mathcal{P}_{a_3}$ and \mathcal{P}_{a_4} , the vertices a_1, \dots, a_5 are represented by a pentagon of the required form and we obtain a regular pentagon contact representation of G . \square

2 Five Color Forests

In this section G will always be an inner triangulation with outer face a_1, \dots, a_5 in clockwise order. The set $1, \dots, 5$ of colors is to be understood as representatives modulo 5, e.g., -1 and 4 denote the same color.

Definition 3. A *five color forest* of G is an orientation and coloring of the inner edges of G in the colors $1, \dots, 5$ with the following properties (see Fig. 3 for an illustration):

(F1) All edges incident to a_i are oriented towards a_i and colored in the color i .

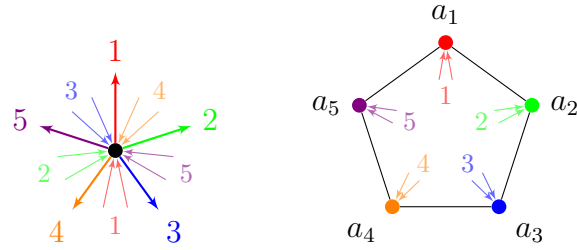


Figure 3: The local conditions of a five color forest

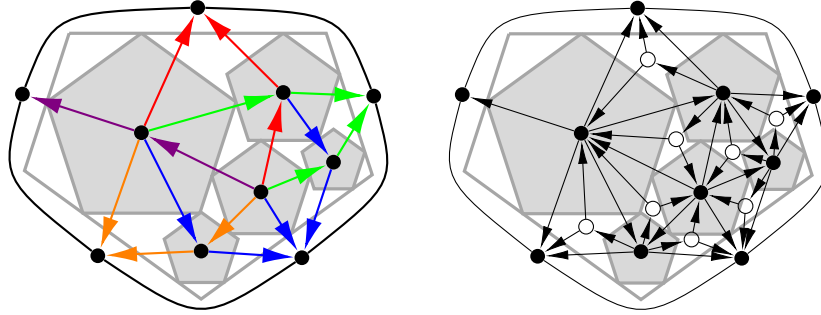


Figure 4: The induced five color forest and α -orientation of a pentagon contact representation.

- (F2) For each inner vertex v , the incoming edges build five (possibly empty) blocks B_i , $i = 1, \dots, 5$, of edges of color i and the clockwise order of these blocks is B_1, \dots, B_5 . Moreover v has at most one outgoing edge of color i and such an edge has to be located between the blocks B_{i+2} and B_{i-2} .
- (F3) For every inner vertex and for $i = 1, \dots, 5$ the block B_i is nonempty or one of the outgoing edges of colors $i - 2$ and $i + 2$ exists.

The following theorem shows the key correspondence between five color forests and pentagon contact representations.

Theorem 4. *Every regular pentagon contact representation induces a five color forest on its contact graph.*

Proof. Let \mathcal{S} be a regular pentagon contact representation of $G = G^*(\mathcal{S})$. We color the corners of all pentagons of \mathcal{S} with the colors $1, \dots, 5$ in clockwise order, starting with color 1 at the corner opposite to the horizontal segment. Let e be an inner edge of G . If e corresponds to the contact of a corner of a pentagon A and a side of a pentagon B in \mathcal{S} , then we orient the edge e from the vertex corresponding to A to the vertex corresponding to B and color it in the color of the corner of A involved in the contact (see Fig. 4 (left)). A contact of two pentagon corners can be interpreted in two ways as a corner-side contact with infinitesimal distance to the other corner. We choose one of these interpretations

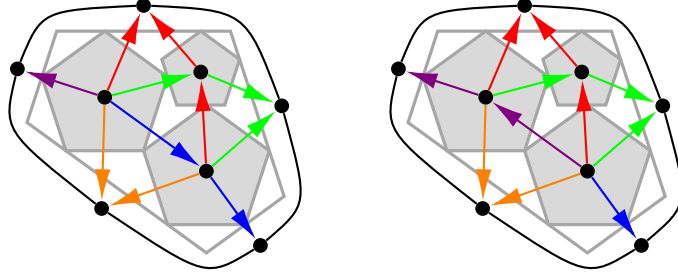


Figure 5: The two induced five color forests of a pentagon contact representation with an exceptional touching.

and proceed as before. Hence, the five color forest induced by a degenerate pentagon contact representation is not unique. Figure 5 shows an example.

We claim that this coloring and orientation of G fulfills the properties of a five color forest. Property (F1) immediately follows from the construction. Now consider property (F2). It is clear that every inner vertex has at most one outgoing edge of every color. That the incoming edges lie in the right interval, follows from the fact that a corner-side contact between two homothetic regular pentagons is only possible if a corner of the first pentagon touches the opposite side of the second pentagon.

Finally we check property (F3) for the case $i = 1$. The other cases are symmetric. Let v be an inner vertex of G and A the corresponding pentagon of \mathcal{S} . Since G is a triangulation, the pentagons corresponding to any two consecutive neighbors of v have to touch. Therefore at least one of these pentagons, we call it B , has to intersect the area below the horizontal side of A , and that is only possible if the contact of A and B corresponds to an incoming edge of v of color 1 or an outgoing edge of color 3 or 4. All other possibilities can be excluded in the following way: If the contact of A and B corresponds to an incoming edge of color 2, then the entire pentagon B lies on the left of the contact point of A and B and therefore also left of the horizontal side of A . If the contact corresponds to an outgoing edge of color 5, each point of B lies above the contact point or on the left of the contact point and therefore above the horizontal side of A or on its left. The other cases can be excluded with similar arguments. \square

Schnyder [15] introduced a similar structure for inner triangulations of a triangle:

Definition 5. A *Schnyder wood* of an inner triangulation T of the triangle b_1, b_2, b_3 is an orientation and coloring of the inner edges of T in the colors 1, 2, 3 with the following properties:

- (S1) All edges incident to b_i are oriented towards b_i and colored in the color i .
- (S2) Each inner vertex has in clockwise order exactly one outgoing edge of color 1, one outgoing edge of color 2 and one outgoing edge of color 3, and in the interval between two outgoing edges there are only incoming edges in the third color.

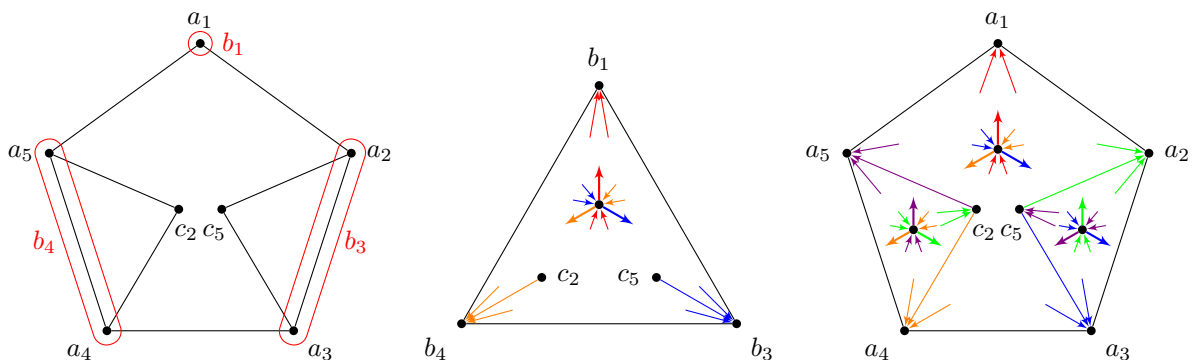


Figure 6: A construction of a five color forest of a given graph using Schnyder woods.

Schnyder proved that every inner triangulation of a triangle admits a Schnyder wood, and using this result, we will show that every inner triangulation of a pentagon admits a five color forest.

Theorem 6 ([15]). *Let T be an inner triangulation of a triangle. Then there exists a Schnyder wood of T .*

Theorem 7. *Let G be an inner triangulation of the pentagon a_1, \dots, a_5 . Then there exists a five color forest of G .*

Proof. The following construction is illustrated by Fig. 6. Contract the edge a_2a_3 to a vertex b_3 and the edge a_4a_5 to a vertex b_4 . In these contraction steps the maximal triangles $c_5a_2a_3$ and $c_2a_4a_5$ incident to a_2, a_3 and to a_4, a_5 are contracted to a single edge, in particular vertices inside these triangles are removed. Further let $b_1 := a_1$. This results in an inner triangulation T of the triangle b_1, b_3, b_4 . Due to Theorem 6 there exists a Schnyder Wood S of T (we use the colors 1, 3, 4 instead of 1, 2, 3).

Take the colors and orientations of all inner edges not inside of $c_5a_2a_3$ or $c_2a_4a_5$ and not incident to a_2 or a_5 from T to G . Now color all inner edges incident to a_2 and not inside $c_5a_2a_3$ in color 2 and orient them towards a_2 , and color all inner edges incident to a_5 and not inside $c_2a_4a_5$ in color 5 and orient them towards a_5 . For the edges inside $c_5a_2a_3$ construct another Schnyder wood where c_5 has incoming edges in color 5, a_3 has incoming edges in color 3, and a_2 has incoming edges in color 2. Analogously, construct a Schnyder wood on the edges inside $c_2a_4a_5$ in the colors 2, 4, 5.

It can easily be verified that this coloring and orientation of the inner edges of G fulfills the properties (F1) and (F2) of a five color forest. To see that property (F3) is also fulfilled we distinguish several cases. If a vertex is not inside $c_5a_2a_3$ or $c_2a_4a_5$ and not adjacent to a_2 or a_5 , it has outgoing edges in colors 1, 3, 4. If a vertex is not inside $c_5a_2a_3$ or $c_2a_4a_5$ and either adjacent to a_2 or to a_5 , it has outgoing edges in colors 1, 2, 4 or 1, 3, 5, respectively. If a vertex is inside $c_5a_2a_3$ or $c_2a_4a_5$, it has outgoing edges in colors 2, 3, 5 or 2, 4, 5, respectively. Therefore in all of these cases property (F3) is fulfilled. The only remaining case is that a vertex v is adjacent to a_2 and a_5 . If $v = c_2 = c_5$, then v has

outgoing edges in all five colors and fulfills property (F3). Otherwise c_2 and c_5 lie inside the 5-gon $a_2a_3a_4a_5v$. Thus this 5-gon is not empty and v has a neighbor w inside this 5-gon (since G has no chords, a_2a_5v cannot be a face of G). Note that the edge between w and v is oriented from w to v and has color 1. Therefore, v has outgoing edges in colors 1, 2, 5 and at least one incoming edge in color 1. Hence, v fulfills property (F3). \square

2.1 α -orientations

Our goal is to connect the setting of five color forests with the well studied orientations of planar graphs with prescribed outdegrees.

Definition 8. Let H be an undirected graph and $\alpha : V(H) \rightarrow \mathbb{N}$. Then an orientation H' of H is called an α -orientation if $\text{outdeg}(v) = \alpha(v)$ for all vertices $v \in V(H')$.

In a five color forest every inner vertex has outdegree at most 5. The following lemma allows us to add vertices and edges so that the outdegree of every inner vertex becomes exactly 5. The statement of the lemma corresponds to the geometric fact that in a regular pentagon contact representation of a triangulation G the area between three pentagons corresponding to a face of G is a quadrilateral with exactly one concave corner.

Lemma 9. *Let G be endowed with a five color forest and let f be a face of G that is incident to at most one outer vertex. Then in exactly one of the three inner angles of f an outgoing edge is missing in the cyclic order of the respective vertex.*

Proof. Since the facial cycle of f has length three, it contains an oriented path of length two. For symmetry reasons we can assume that this path is oriented clockwise and the first edge of this path has color 1. Then because of property (F3) the second edge of this path can only have the colors 2 and 3. Figure 7 shows all possible cases for the orientation and coloring of the third edge of the cycle and verifies the statement for all these cases. \square

Now we define an extension of G and a function α_5 such that every five color forest of G can be extended to an α_5 -orientation of this extension.

Definition 10. The *stack extension* G^* of G is the extension of G that contains an extra vertex in every inner face that is incident to at most one of the outer vertices. These new vertices are connected to all three vertices of the respective face (see Fig. 4 (right)). We call the new vertices *stack vertices* and the vertices of G *normal vertices*.

Definition 11. An orientation of the inner edges of G^* is a α_5 -orientation if the outdegrees of the vertices correspond to the following values:

$$\alpha_5(v) = \begin{cases} 2 & \text{if } v \text{ is a stack vertex,} \\ 5 & \text{if } v \text{ is an inner normal vertex,} \\ 0 & \text{if } v \text{ is an outer normal vertex.} \end{cases}$$

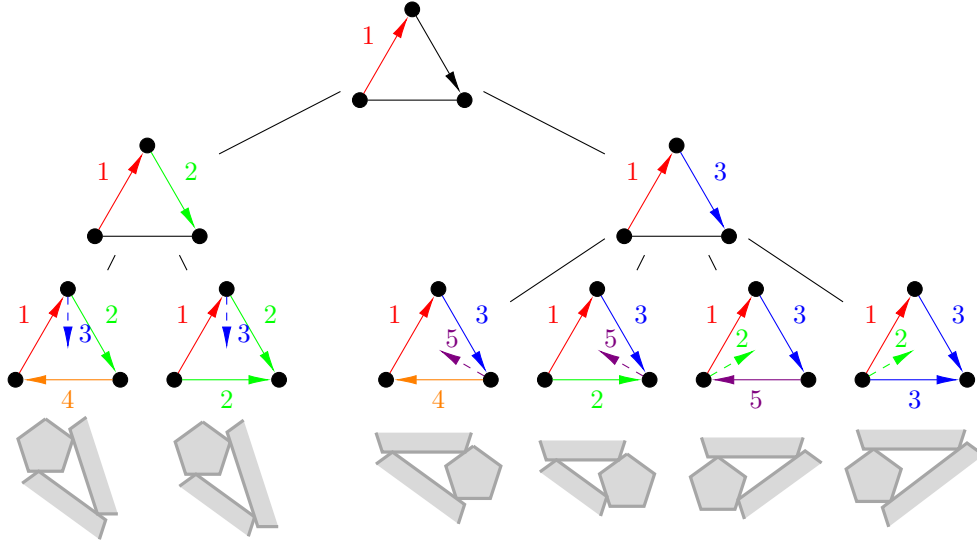


Figure 7: Full case distinction for Lemma 9

A five color forest of G induces an α_5 -orientation of G^* in a canonical way by keeping the orientation of the edges of G and defining the missing edge of Lemma 9 as the unique incoming edge for every stack vertex.

Observation 12. *The coloring of the inner edges of a five color forest can be extended to a coloring of the inner edges of the induced α_5 -orientation that fulfills the properties of a five color forest at all normal vertices.*

2.2 Bijection between five color forests and α_5 -orientations

Now we want to prove that the canonical mapping from five color forests to α_5 -orientations is a bijection. For this purpose we need to reconstruct the colors of the inner edges of G if we are given an α_5 -orientation. The idea of this construction will be to start with an inner edge e of G and follow a properly defined path until it reaches one of the five outer vertices. Then the color of this outer vertex will be the color of e . This approach is similar to the proof of the bijection of Schnyder Woods and 3-orientations in [4].

Lemma 13. *Let C be a simple cycle of length ℓ in G^* and let all vertices of C be normal vertices, i.e., vertices of G . Then there are exactly $2\ell - 5$ edges pointing from C into the interior of C .*

Proof. First we view C as a cycle in G . Let k be the number of vertices strictly inside C . Since G is an inner triangulation there are exactly $2k + \ell - 2$ faces and $3k + \ell - 3$ edges strictly inside C by Euler's formula.

Now we view C as a cycle in G^* . In addition to the $3k + \ell - 3$ normal edges there are 3 stack edges in each face, hence, the number of edges in C is $9k + 4\ell - 9$. At each stack vertex we see 2 starting edges and at every normal vertex 5. Therefore there are

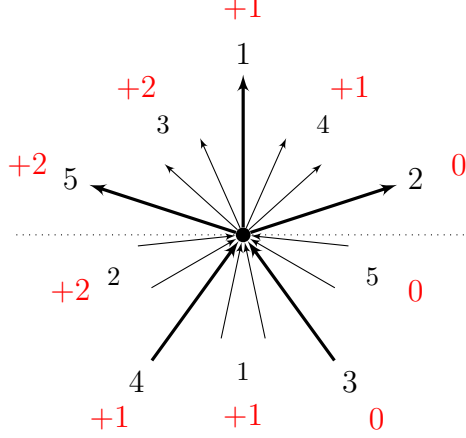


Figure 8: The possible incident edges of a vertex v in T . For an incoming edge of color c below the dotted line the red value is $2 - \pi(c)$ and counts the number of thick edges in the counterclockwise angle from this edge to the dotted line. For an outgoing edge of color c' above the dotted line the red value is $\pi(c')$ and counts the number of thick edges in the clockwise angle from this edge to the dotted line. The thick edges are exactly those that are outgoing in v in the α -orientation.

$2(2k + \ell - 2) + 5k = 9k + 2\ell - 4$ edges starting at a vertex inside C . Taking the difference we find that there are $2\ell - 5$ edges pointing from a vertex of C into the interior. \square

Next we will show some properties of oriented cycles in five color forests. By T_i we denote the forest consisting of all edges of color i , and by T_i^{-1} we denote the forest T_i with all edges reversed.

Lemma 14. *The orientation $T := T_i + T_{i-1} + T_{i+1} + T_{i-2}^{-1} + T_{i+2}^{-1}$ of G is acyclic.*

Proof. Assume there is a simple oriented cycle C of length ℓ in T . Because of the symmetry of the colors in the definition of a five color forest, it suffices to consider the case that C is oriented clockwise and $i = 1$.

We define the following auxiliary function for the five colors:

$$\pi(1) := 1 \quad , \quad \pi(2) := 0 \quad , \quad \pi(3) := 2 \quad , \quad \pi(4) := 1 \quad , \quad \pi(5) := 2 \quad .$$

Let e be an edge of color c ending at vertex v and e' an edge of color c' starting at v in the orientation T . From Fig. 8 we can read off the following: In the counterclockwise angle of v between e and the dotted line there are $2 - \pi(c)$ edges which are outgoing in the α_5 -orientation of G^* . In the clockwise angle of v between e' and the dotted line there are $\pi(c')$ outgoing edges. Hence, there are exactly $\pi(c') + (2 - \pi(c))$ edges pointing away from v in the counterclockwise angle between e and e' (in the α_5 -orientation of G^*).

Now let e_1, \dots, e_ℓ be the edges of the cycle C of T and let c_i be the color of edge e_i . Then the number of edges pointing from C into the interior (in the α_5 -orientation of G^*)

is

$$\sum_{i=1}^{\ell-1} (\pi(c_{i+1}) - \pi(c_i) + 2) + (\pi(c_1) - \pi(c_\ell) + 2) = 2\ell .$$

This is in contradiction to Lemma 13. \square

Proposition 15. *Let C be an oriented cycle in G where G is oriented with every T_i . Then:*

- (i) C uses at least 3 different colors.
- (ii) If C uses exactly 3 different colors, these colors are not consecutive in the cyclic order.
- (iii) C has two consecutive edges whose colors have distance at most one in the cyclic order.

Proof. For the first two statements we denote by J the set of colors used by C . Assume that $|J| \leq 2$ or $|J| = \{j, j+1, j+2\}$ for a color j . In both cases there is a color i such that $J \subseteq \{i, i-1, i+1\}$ (in the second case we choose $i = j+1$). Thus C is an oriented cycle in the orientation $T_i + T_{i-1} + T_{i+1} + T_{i-2}^{-1} + T_{i+2}^{-1}$, in contradiction to Lemma 14.

For the third statement assume that there is an oriented simple cycle C such that the distance of the colors of any two consecutive edges on C is exactly 2. Because of the symmetry it suffices to consider the case that C is oriented clockwise. Let $e = uv$ and $e' = vw$ be two consecutive edges on C and let i be the color of e . If the color of e' is $i+2$, there is no edge pointing from v into the interior of C , i.e., there is no outgoing edge of v in the interval between the edges e' and e in the clockwise cyclic order of the incident edges of v . If the color of e' is $i-2$, there are exactly 4 edges pointing from v into the interior of C . Therefore the total number of edges pointing into the interior of C is even, in contradiction to Lemma 13. \square

Now we will define the paths starting with an inner edge e and ending at an outer vertex that allow us to define the color of e . The idea is to always continue with the opposite outgoing edge, but if we run into a stack vertex, we need to be careful. The paths we will define are not unique, but we will see that all paths starting with the same edge e end at the same outer vertex.

Definition 16. Let $e = uv$ be an inner edge such that u is a normal vertex. We will recursively define a set $\mathcal{P}(e)$ of walks starting with e by distinguishing several cases concerning v .

- If v is an outer vertex, i.e., $v = a_i$ for some i , the set $\mathcal{P}(e)$ contains only one path, the path only consisting of the edge e .
- If v is an inner normal vertex, let e' be the opposite outgoing edge of e at v , i.e., the third outgoing edge in clockwise or counterclockwise direction, and we define $\mathcal{P}(e) := \{e + P : P \in \mathcal{P}(e')\}$.

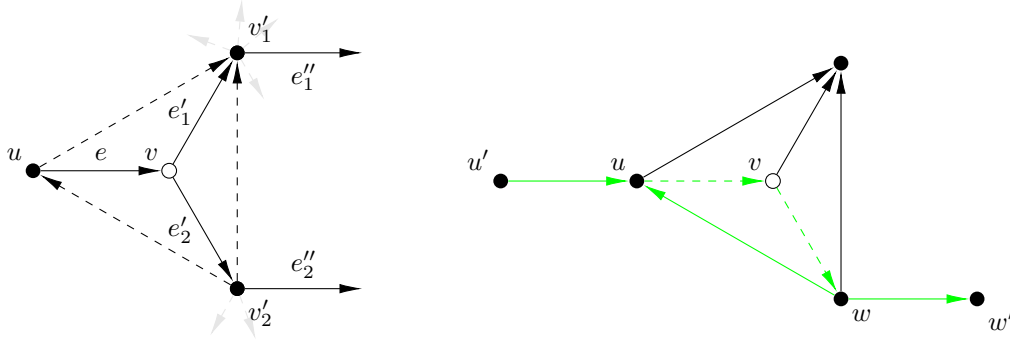


Figure 9: Left: An example for the third case in the definition of the set $\mathcal{P}(e)$ of walks. Right: An example for the construction of the shortcut walk: The stack edges uv and vw of the walk (u', u, v, w, w') are replaced by the edge uw in the shortcut walk (u', u, w, w') . In the α_5 -orientation this edge is oriented from w to u .

- If v is a stack vertex, let $e'_1 = vv'_1$ and $e'_2 = vv'_2$ be the left and right outgoing edge of v . Further let e''_1 be the second outgoing edge of v'_1 after e'_1 in counterclockwise direction and e''_2 the second outgoing edge of v'_2 in clockwise direction. Note that e''_i is well defined if v'_i is not an outer vertex, and that not both of v'_1 and v'_2 can be outer vertices (there are no stack vertices in faces of G that are incident to two outer vertices). If both of e''_1 and e''_2 are well defined, we define $\mathcal{P}(e) := \{e + e'_1 + P : P \in \mathcal{P}(e''_1)\} \cup \{e + e'_2 + P : P \in \mathcal{P}(e''_2)\}$. If only e''_i is well defined, we define $\mathcal{P}(e) := \{e + e'_i + P : P \in \mathcal{P}(e''_i)\}$. See Fig. 9 (left) for an example.

At the moment it is not clear that these walks are finite. If they are finite, they have to end in an outer vertex. But we have to prove that they do not cycle.

Lemma 17. (i) *The walks $P \in \mathcal{P}(e)$ are paths, i.e., there are no vertex repetitions in P .*

(ii) *Let $P_1, P_2 \in \mathcal{P}(e)$ be two paths starting with the same edge e . Then P_1 and P_2 end in the same outer vertex.*

(iii) *Let v be a normal vertex and let $e_1 = vv_1, e_2 = vv_2$ be two different outgoing edges at v . Further let $P_1 \in \mathcal{P}(e_1)$ and $P_2 \in \mathcal{P}(e_2)$ be two paths. Then P_1 and P_2 do not cross and they end in different outer vertices.*

Before we can prove Lemma 17, we have to introduce some notations. The general approach for the proof will be to produce contradictions to Lemma 13. Since Lemma 13 is a statement about cycles only consisting of normal vertices and the walks considered in Lemma 17 consist of normal and stack vertices, we consider abbreviations of these walks only consisting of normal vertices.

Definition 18. For a given edge e let P be a finite subwalk of a walk in $\mathcal{P}(e)$ that starts and ends with a normal vertex. Then the *shortcut* P' of P is obtained from P

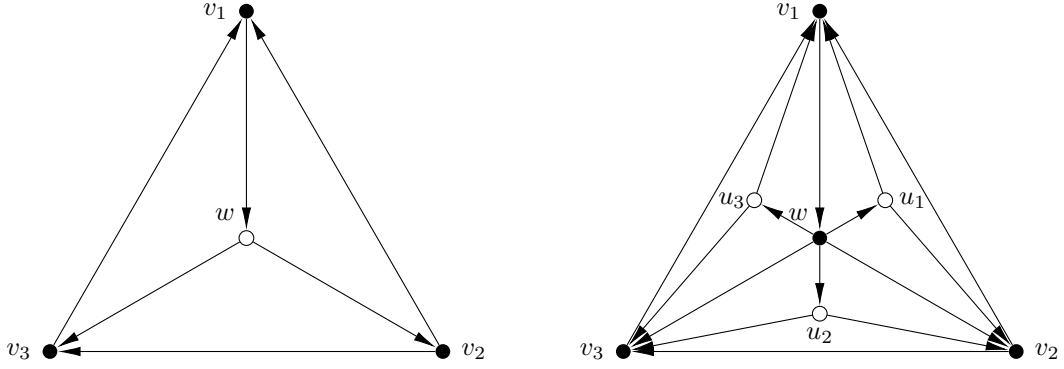


Figure 10: An example for stacking a normal vertex into a face of G .

by replacing every consecutive pair uv, vw of edges, where v is a stack vertex, by the edge uw . We call uw a *shortcut edge*. Note that this edge might be oriented from w to u in the α_5 -orientation, and thus shortcut walks in general are not oriented walks in the α_5 -orientation. See Fig. 9 (right) for an example.

Let P be a finite subwalk of a walk defined in Definition 16. For our later argumentation we need to be able to extend such a walk P by a normal edge before its first edge or after its last edge such that the extended walks remains a subwalk of a walk defined in Definition 16. For sure, P has to start or to end with a normal vertex, respectively, to allow such an extension. Since this condition is not sufficient, we have to change the graph G in some cases. Thus we can find the contradictions to Lemma 13 in the new graph.

Definition 19. Let X be a fixed α_5 -orientation of G^* . Let w be a stack vertex and let v_1, v_2, v_3 be its neighbors in G^* such that in X the edge v_1w is incoming at w and the edges wv_2, wv_3 are outgoing at w . Then we call the following change of G, G^* and X *stacking a normal vertex at w* : The vertex w becomes a normal vertex and we add stack vertices u_1, u_2, u_3 in the three incident faces of w . All edges keep their orientations, the edges wu_i are incoming at the u_i and the edges u_iv_j are outgoing at the u_i . See Fig. 10 for an example.

Note that after stacking a normal vertex at w the walks defined in Definition 16 change in the following way: After each occurrence of w the vertex u_2 is inserted. If a walk does not contain the vertex w , it remains the same.

Lemma 20. *Let P be a finite subwalk of a walk defined in Definition 16 that starts (ends) with an inner normal vertex. Then after stacking at most two normal vertices, P can be extended by a normal edge before its first edge (after its last edge) in such a way that it remains a subwalk of a walk defined in Definition 16.*

Proof. Let $P = v_1, v_2, \dots, v_n$. Let us first consider the case that v_1 is a normal vertex and that we want to extend P by a normal edge v_0v_1 . We distinguish three cases. In

the first case v_1 has an incoming normal edge v_0v_1 such that v_1v_2 is the third outgoing edge of v_1 in clockwise (and counterclockwise) order after v_0v_1 . Then we are done because due to Definition 16 (second case) v_1v_2 is the unique successor of v_0v_1 . In the second case v_1 has an incoming stack edge v_0v_1 such that v_1v_2 is the third outgoing edge of v_1 in clockwise (and counterclockwise) order after v_0v_1 . Then we can stack a normal vertex at v_0 and we are in the first case, again. In the third case v_1 has no incoming edge v_0v_1 such that v_1v_2 is the third outgoing edge of v_1 in clockwise (and counterclockwise) order after v_0v_1 . Then v_1 has an outgoing stack edge v_1w and an outgoing normal edge v_1w' such that v_1v_2 is the second outgoing edge of v_1 either in clockwise or in counterclockwise order after v_1w and after v_1w' since the neighbors of v_1 alternate between normal vertices and stack vertices. If we stack a normal vertex at w , a stack vertex u is stacked into the face v_1ww' of G^* . Since the edge uv_1 is incoming at v_1 , we are in the second case, again.

Now let us consider the case that v_n is an inner normal vertex and that we want to extend P by a normal edge v_nv_{n+1} . Due to Definition 16 (second and third case) there is exactly one outgoing edge v_nv_{n+1} of v_n such that the extended walk v_1, \dots, v_{n+1} is a subwalk of a walk defined in Definition 16. If v_{n+1} is a normal vertex, we are done. Otherwise we stack a normal vertex at v_{n+1} and are also done. \square

If P is a path with designated start vertex s , then at an inner vertex v we can distinguish edges on the right side of P and edges on the left side of P . We define $\text{r-out}_P(v)$ and $\text{l-out}_P(v)$ to be the number of right and left outgoing edges from path P at vertex v , respectively.

Lemma 21. *Let P' be a shortcut walk of length ℓ that does not start and does not end with a shortcut edge. Then the number of edges pointing from the inner vertices of P' to the right (left) of P' is $2(\ell - 1)$.*

Proof. Since right and left are symmetric, it is enough to prove the lemma for right outgoing edges. The proof is by induction on the length ℓ of the walk. If $\ell = 2$, the shortcut walk is equal to the original walk and consists of two normal edges since by assumption the shortcut walk does not start and does not end with a shortcut edge. Due to Definition 16 (second case) this path has $2 = 2(\ell - 1)$ outgoing edges on either side. Now let $\ell \geq 3$ and let $P' = v_0, e_1, v_1, \dots, e_\ell, v_\ell$. If $e_{\ell-1}$ is not a shortcut edge, the statement follows by induction because the vertex between two consecutive normal edges of a walk in $\mathcal{P}(e)$ has 2 outgoing edges on either side by Definition 16 (second case).

Now assume that $e_{\ell-1}$ is a shortcut edge and let $e' = v_{\ell-2}w, e'' = wv_{\ell-1}$ be the corresponding edges of the original path P . Let Q' be the subwalk of P' starting at v_0 and ending at $v_{\ell-2}$ extended by the edge $v_{\ell-2}w$. Note that we can apply the induction hypothesis to Q' by stacking a normal vertex at w . Hence, we know that the number of edges pointing from an inner vertex of Q' to the right is $2(\ell - 2)$.

The edges $v_{\ell-2}w$ and $v_{\ell-2}v_{\ell-1}$ are consecutive in the cyclic order of incident edges of $v_{\ell-2}$. Define a sign σ to be -1 if $v_{\ell-2}v_{\ell-1}$ is right of $v_{\ell-2}w$ and $+1$ otherwise. Let $\delta = 0$ if $\sigma = -1$ and $v_{\ell-2}v_{\ell-1}$ is outgoing at $v_{\ell-1}$, otherwise $\delta = 1$. When comparing outgoing edges at $v_{\ell-2}$ in P' and Q' the contribution of δ will account for the edge $v_{\ell-2}v_{\ell-1}$ if $\sigma = -1$

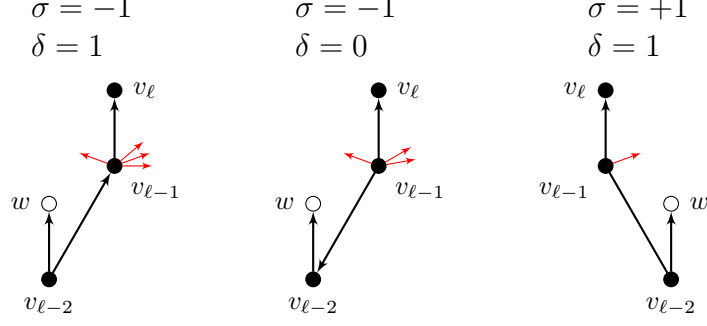


Figure 11: Right outgoing edges at v_{l-2} and v_{l-1} .

(if $\delta = 1$ and $\sigma = -1$, the edges pointing from v_{l-2} to the right of P' are exactly the edges pointing from v_{l-2} to the right of Q' minus the edge $v_{l-2}v_{l-1}$) and for the edge $v_{l-2}w$ if $\sigma = +1$ (if $\delta = 1$ and $\sigma = +1$, the edges pointing from v_{l-2} to the right of P' are exactly the edges pointing from v_{l-2} to the right of Q' plus the edge $v_{l-2}w$). It follows that $\text{r-out}_{P'}(v_{l-2}) = \text{r-out}_{Q'}(v_{l-2}) + \sigma\delta$, see Fig. 11.

Claim 1. $\text{r-out}_{P'}(v_{l-1}) = 2 - \sigma\delta$.

Proof. If $\sigma = +1$, then we are in the v'_1 case of the stack vertex part in Definition 16, i.e., between $v_{l-2}v_{l-1}$ and $v_{l-1}v_l$ there is one outgoing edge on the right at v_{l-1} . The claim follows because in this case $\delta = 1$.

If $\sigma = -1$, then we are in the v'_2 case of the stack vertex part in Definition 16, i.e., between $v_{l-2}v_{l-1}$ and $v_{l-1}v_l$ there is one outgoing edge on the left at v_{l-1} . Now it depends on whether the edge $v_{l-2}v_{l-1}$ is outgoing at v_{l-2} or at v_{l-1} . In the first case we have $\delta = 1$ and $\text{r-out}_{P'}(v_{l-1}) = 3$, in the second case $\delta = 0$ and $\text{r-out}_{P'}(v_{l-1}) = 2$. In either case this is what the claim says. \triangle

The number of right outgoing edges of P' is obtained as the sum of those of Q' , which is $2(\ell - 2)$, with $\text{r-out}_{P'}(v_{l-2}) - \text{r-out}_{Q'}(v_{l-2})$, which is $\sigma\delta$, and $\text{r-out}_{P'}(v_{l-1})$, which is $2 - \sigma\delta$ by Claim 1. Hence, the number of right outgoing edges of P' is $2(\ell - 1)$. \square

Lemma 22. *Let P' be a shortcut walk of length ℓ (that might start or end with a shortcut edge). Then the number of edges pointing from the inner vertices of P' to the right (left) of P' is $2(\ell - 1) + \mu$ with $-2 \leq \mu \leq 2$.*

Proof. Because of symmetry it is enough to proof the lemma for the right outgoing edges of P' . Let P be the original walk. Further let Q be the walk P extended by a normal edge at both ends (possibly after stacking normal vertices). We denote the shortcut of Q by $Q' = v_{-1}, e_0, v_0, e_1, v_1, \dots, e_\ell, v_\ell, e_{\ell+1}, v_{\ell+1}$. Due to Lemma 21 there are exactly $2(\ell + 1)$ edges pointing from the inner vertices of Q' to the right of Q' . From Claim 1 in the proof of Lemma 21 (see also Fig. 11) it follows that there are $\mu_1 \in \{1, 2, 3\}$ edges pointing from v_ℓ to the right of Q' . With a similar case distinction (see Fig. 12) we can see that there are $\mu_2 \in \{1, 2, 3\}$ edges pointing from v_0 to the right of Q' . Therefore there are

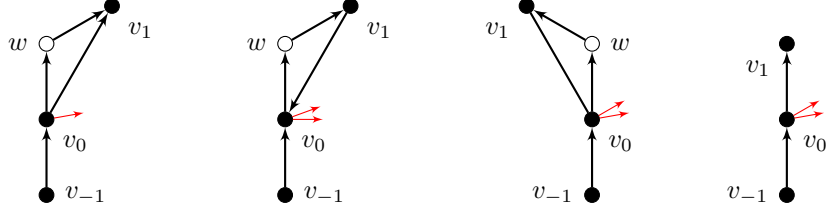


Figure 12: Right outgoing edges at v_0 .

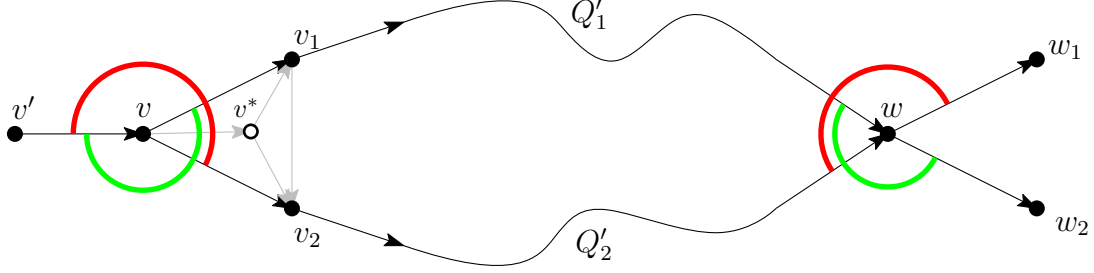


Figure 13: Overcounts at the two ends of the paths Q'_1 and Q'_2 . Edges in the green area are counted as right edges of Q'_1 , those in the red area as left edges of Q'_2 .

exactly $2(\ell + 1) - \mu_1 - \mu_2 = 2(\ell - 1) + (4 - \mu_1 - \mu_2)$ edges pointing from the inner vertices of P' to the right of P' . Since $-2 \leq 4 - \mu_1 - \mu_2 \leq 2$, this completes the proof. \square

Now we are ready to prove Lemma 17.

Proof of Lemma 17. For (i) assume that P cycles. Let C be a simple cycle which appears as a subwalk of the shortcut of P , and let ℓ be its length. According to Lemma 22, there are at least $2(\ell - 1) - 2$ edges pointing into the interior of C . This is in contradiction to Lemma 13 which states that there are only $2\ell - 5$ edges pointing into the interior of C .

For (ii) assume that P_1 and P_2 coincide up to a vertex v^* , then P_1 goes to the left and P_2 to the right. Note that v^* has to be a stack vertex and let v and v' be its predecessors in P_1 and P_2 , i.e., v', v, v^* appear in this order on both paths. If P_1 and P_2 start in v , we can use a dummy edge $v'v$ (possibly after stacking normal vertices) which makes sure that $\text{r-out}_{P_1}(v) = \text{l-out}_{P_2}(v) = 2$. For $i = 1, 2$ let P'_i be the shortcut of P_i .

Claim 1. $\text{r-out}_{P'_1}(v) + \text{l-out}_{P'_2}(v) = 6$.

Proof. Every outgoing edge of v except possibly the edge vv' is a right edge with respect to P'_1 or a left edge with respect to P'_2 . The edge from v to v^* is both and therefore counted twice, see Fig. 13 (left). \triangle

Claim 2. *If after splitting at v the two shortcut paths P'_1 and P'_2 meet at some vertex w which is not an outer vertex, then the first vertex w' after w is the same on P_1 and P_2 .*

Proof. For $i = 1, 2$ let Q'_i be the subpath of P'_i starting at v and ending at w . At the beginning these paths are extended by a normal edge $v'v$ (possibly after stacking normal vertices). At the end the paths are extended by the successor w_i of w on P_i . If w_i is a stack vertex, we can pretend that it is a normal vertex by stacking a normal vertex at w_i .

Let ℓ_i be the length of Q'_i . From Lemma 21 we know that there are exactly $2(\ell_1 - 1)$ edges pointing from Q'_1 to the right and exactly $2(\ell_2 - 1)$ edges pointing from Q'_2 to the left. Let C be the cycle formed by the two shortcuts Q'_1 and Q'_2 between v and w . The length of C is $\ell_1 + \ell_2 - 4$ (C consists of the edges of Q'_1 and Q'_2 except for their first and last edges) and therefore, by Lemma 13, there are exactly $2(\ell_1 + \ell_2 - 4) - 5$ edges pointing into the interior of C .

The sum of the right edges of Q'_1 and the left edges of Q'_2 correctly accounts for the edges pointing into the interior of C at all vertices except at v and w . Claim 1 implies that at v we overcount by exactly 5, i.e., the number of edges pointing from Q'_1 to the right plus the number of edges pointing from Q'_2 to the left is 6, but at v only 1 edge is pointing into the interior of C . It follows that the overcount at w is

$$(2(\ell_1 - 1) + 2(\ell_2 - 1)) - (2(\ell_1 + \ell_2 - 4) - 5) - 5 = 4 ,$$

where $2(\ell_1 - 1) + 2(\ell_2 - 1)$ is the number of edges pointing from Q'_1 to the right plus the number of edges pointing from Q'_2 to the left, $2(\ell_1 + \ell_2 - 4) - 5$ is the number of edges pointing into the interior of C and 5 is the overcount at v . This means that each edge except one contributes to the overcount at w , see Fig. 13 (right). Hence, ww_1 and ww_2 have to be identical and $w' = w_1 = w_2$. \triangle

Now suppose that P_1 and P_2 end at different outer vertices a_i and a_j . Let v^* be the last common vertex of the two paths, v^* has to be a stack vertex. Assume that P_1 goes to the left at v^* and P_2 goes to the right. Let v be the predecessor of v^* in P_1 and P_2 . Further let Q_1 and Q_2 be the subpaths of P_1 and P_2 starting at v and ending at a_i and a_j , extended by a normal edge $v'v$ (possibly after stacking normal vertices). For $i = 1, 2$ let Q'_i be the shortcut of Q_i and let $\ell_i + 1$ be the length of Q'_i . Let $\ell_3 \geq 2$ be the length of the path P_3 between a_i and a_j that alternates between outer and inner normal vertices. Note that P_3 has $\frac{\ell_3}{2}$ inner vertices and $\frac{\ell_3}{2} + 1$ outer vertices. Let C be the simple cycle in the union of Q'_1 , Q'_2 and P_3 . Note that P_3 can have at most one common edge with each Q'_i . Let $\xi \in \{0, 1, 2\}$ be the number of common edges of P_3 with $Q'_1 \cup Q'_2$. The length of C is $\ell_1 + \ell_2 + \ell_3 - 2\xi$. If $\xi = 0$ the edges pointing into C can be obtained by adding the right edges of Q'_1 and the left edges of Q'_2 subtracting 5 for the overcount at v and adding 3 for each normal vertex of P_3 . When Q'_1 shares the last edge with P_3 , then we have to disregard the contribution of the first normal vertex w of P_3 and subtract one for the edge wa_{i+1} which belongs to C and is counted as a right edge of Q'_1 . Hence, we obtain the following estimate for the number of edges pointing into C :

$$2\ell_1 + 2\ell_2 - 5 - \xi + 3\left(\frac{\ell_3}{2} - \xi\right) = 2(\ell_1 + \ell_2 + \ell_3 - 2\xi) - 5 - \frac{\ell_3}{2} .$$

This is less than the number of edges pointing into C which is $2(\ell_1 + \ell_2 + \ell_3 - 2\xi) - 5$ by Lemma 13. See Fig. 14 for an illustration.

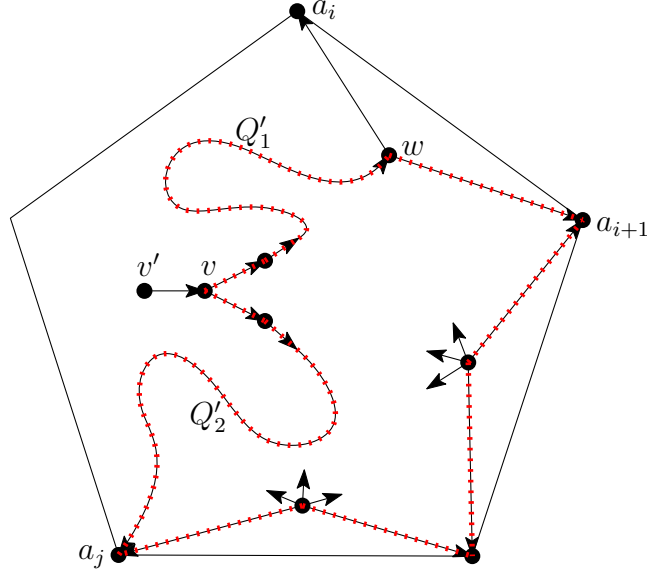


Figure 14: Illustration of the proof of Lemma 17 (ii). The cycle C is drawn in red and dotted. The edge wa_i is contained in Q'_1 and in P_3 . Therefore this is the case $\xi = 1$.

For (iii) assume that P_1 and P_2 have a common vertex different from v and let w be the first normal vertex of this kind (note that P_1 and P_2 might already meet at a stack vertex immediately before w). Let Q_1 and Q_2 be the subpaths of P_1 and P_2 that begin with the predecessors v'_1 and v'_2 of v , respectively, and end with the successors w_1 and w_2 of w , respectively. After possibly stacking some normal vertices, we can assume that v'_1, v'_2 exist and that v'_1, v'_2, w_1, w_2 are normal vertices. Let Q'_1 and Q'_2 be the corresponding shortcut paths and let ℓ_1 and ℓ_2 be their lengths. Note that the successor edge of v in Q_i and Q'_i is the same. Let C be the cycle we get by gluing the parts of Q'_1 and Q'_2 between v and w together. Let s be the number of outgoing edges of v between Q'_1 and Q'_2 inside C . We assume that looking from v into the interior of C , the left edge of C belongs to Q'_1 and the right one to Q'_2 . The number of outgoing edges between v'_2v and v'_1v is $5 - (\text{r-out}_{Q_1}(v) + \text{l-out}_{Q_2}(v) - s) = s + 1$. The length of C is $\ell_1 + \ell_2 - 4$ and therefore, due to Lemma 13, exactly $2(\ell_1 + \ell_2 - 4) - 5$ edges are pointing into the interior of C . If we add the number of edges pointing from Q'_1 to the right and the number of edges pointing from Q'_2 to the left, we overcount by $5 - (s + 1)$ at v . Hence, the overcount at w must be

$$(2(\ell_1 - 1) + 2(\ell_2 - 1)) - (5 - (s + 1)) - (2(\ell_1 + \ell_2 - 4) - 5) = 5 + s .$$

To get an overcount ≥ 5 at w we need to have every edge in the union of the right edges of Q'_1 and left edges of Q'_2 . In particular ww_1 is to the left of Q'_2 . This implies that at least one of the edges of Q'_1 and Q'_2 ending in w must be a shortcut edge. It follows that w is not an outer vertex. Further there are exactly s outgoing edges of w between ww_1 and ww_2 . Therefore we can inductively repeat the argument for the subpaths of P_1 and P_2 starting at w . See Fig. 15 for an illustration. \square

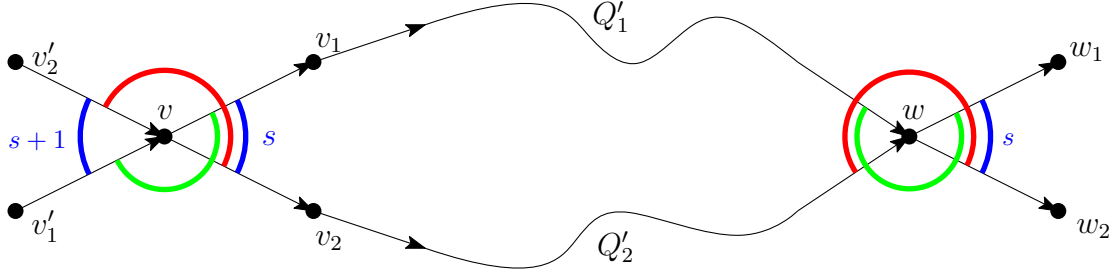


Figure 15: Illustration of the proof of Lemma 17 (iii). The outgoing edges in the green (red) angles are the edges pointing from Q'_1 to the right (from Q'_2 to the left). In the blue angles there are s or $s + 1$ outgoing edges.

Now we are able to prove the main result of this subsection.

Theorem 23. *The canonical map from five color forests to α_5 -orientations is a bijection.*

Proof. Let \mathcal{F} be the set of five color forests of G and \mathcal{A} the set of α_5 -orientations of G^* . Further let $\chi : \mathcal{F} \rightarrow \mathcal{A}$ be the canonical map and $\psi : \mathcal{A} \rightarrow \mathcal{F}$ the map that keeps the orientation of the edges as in the α_5 -orientation and colors every edge e in the color of the end vertex of the paths in $\mathcal{P}(e)$.

Claim 1. *The map $\psi : \mathcal{A} \rightarrow \mathcal{F}$ is well-defined.*

Proof. Lemma 17 (i) and (ii) show that ψ is a well-defined coloring of the edges of G . It remains to show that this coloring fulfills the properties of a five color forest.

Property (F1) is clear from the construction.

Now consider property (F2). Because of Lemma 17 (iii) the circular order of the colors of the outgoing edges of an inner vertex has to coincide with the order of the colors of the outer vertices. That the incoming edges of color i are opposite of the outgoing edge of the same color i , follows from the construction of the paths.

For showing property (F3) assume that there is an inner vertex v with no outgoing edges of colors $i - 2$ and $i + 2$ for some i . In the α_5 -orientation these missing outgoing edges correspond to edges ending in stack vertices. In the interval between these two outgoing edges there has to be at least one edge $e = vw$ with a normal vertex w . And because of property (F2) this edge can only be an incoming edge and the color is i . \triangle

Claim 2. *The function $\psi : \mathcal{A} \rightarrow \mathcal{F}$ is injective.*

Proof. We show that we can recover the edges of G^* from the five color forest on G .

The orientation at normal vertices can directly be read of from the five color forest. Lemma 9 implies that the orientation at stack edges is also prescribed by the five color forest. \triangle

Claim 3. *The function $\chi : \mathcal{F} \rightarrow \mathcal{A}$ is injective.*

Proof. We show that we can recover the coloring of the edges of a five color forest from the orientations of the edges, i.e., from the α_5 -orientation in the image of χ .

Clearly, the colors of the edges incident to the outer vertices are known. Moreover, because of property (F2) the knowledge of the color of a normal edge incident to an inner normal vertex v implies the knowledge of the colors of all edges incident to v . Since G is connected, this implies that the colors of all edges are unique and known. \triangle

Since \mathcal{A} and \mathcal{F} are finite sets, and $\chi \circ \psi$ is the identity map on α_5 -orientations, we obtain from Claims 2 and 3 that ψ and χ are inverse bijections. \square

2.3 The distributive lattice of five color forests

It has been shown in [6] that the set of all α -orientations of a planar graph carries the structure of a distributive lattice. We need some definitions to be able to describe the cover relation of this lattice.

Definition 24. A *chordal path* of a simple cycle C is a directed path consisting of edges inside C whose first and last vertex are vertices of C . These two vertices are allowed to coincide.

Definition 25. A simple cycle C is an *essential cycle* if there is an α -orientation X such that C is a directed cycle in X and has no chordal path in X .

Theorem 26 ([6]). *The following relation on the set of all α -orientations of a planar graph is the cover relation of a distributive lattice: An α -orientation X covers an α -orientation Y if and only if X can be obtained from Y by the reorientation of a counterclockwise oriented essential cycle in Y .*

The reorientation of a counterclockwise (clockwise) oriented essential cycle is called a *flip (flop)*. The following theorem gives a full characterization of the flip operation in the lattice of five color forests.

Theorem 27. *The set of all α_5 -orientations on G^* carries the structure of a distributive lattice. The flip operation in this lattice is the reorientation of a counterclockwise oriented facial cycle.*

Proof. Let C be an essential cycle in G^* . Then there exists an α_5 -orientation X such that C is a directed cycle in X and has no chordal path in X . Suppose that C is not facial.

Claim 1. *There is no edge pointing into the interior of C .*

Proof. Assume that there is an edge e pointing from a normal vertex into the interior of C . Let $P \in \mathcal{P}(e)$ be a directed path starting with the edge e and ending in an outer vertex of G^* . Then P has to cross C at some point and the subpath of P that ends at the first crossing vertex with C is a chordal path of C , contradicting that C is essential.

If $e = vw$ is a stack edge, then v is a stack vertex and w a normal vertex. If w is on C , the edge e is a chord of C . Otherwise take any outgoing edge e' of w , then a path $P \in \mathcal{P}(e')$ has to cross C . Together with e this yields a chordal path. \triangle

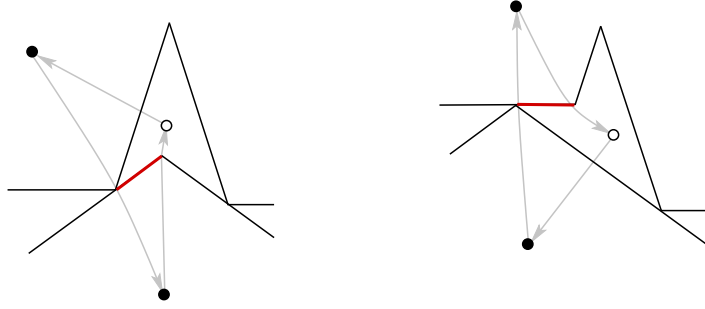


Figure 16: A flip of a facial cycle in an α_5 -orientation and its effect on contacts of pentagons. The red segment contributes to another pentagon.

Claim 2. *The cycle C contains at least one stack vertex.*

Proof. Assume that C contains only normal vertices. Then according to Lemma 13 there are exactly $2\ell(C) - 5 \neq 0$ edges pointing into the interior of C , in contradiction to Claim 1. \triangle

Now let v be a stack vertex on C . Let w_1 be the predecessor and w_2 be the successor of v on C . We know that the other outgoing edge of v has to point to the outside of C . Now, unless C is a facial cycle the edge w_1w_2 is an inner chord of C . In either orientation the edge forms a chordal path, hence, C is not essential. \square

Figure 16 shows the effect of a flip in terms of contacts of pentagons, the effect on the five color forest can be read from the figure.

3 The Algorithm

In this section we will propose an algorithm to compute a regular pentagon contact representation of a given graph G .

We will propose a system of linear equations related to a given five color forest F of G . If the five color forest is induced by a regular pentagon representation, the solution of the system allows to compute coordinates for the corners of the pentagons in this representation. Otherwise the solution of the system will have negative variables.

We start by describing how to obtain the skeleton graph G_{skel} of the contact representation from the given five color forest F . We start with a crossing-free straight-line drawing of G . Add a subdivision vertex on each edge of G . Moreover, for each inner vertex v draw an edge ending at a new vertex inside each face with a missing outgoing edge of v . Then connect all the new adjacent vertices of v in the cyclic order given by the drawing. We call the resulting polygon the *abstract pentagon* of v (note that this polygon can have more than five corners). Since, due to Lemma 9, in each face of G which is incident to at most one outer vertex there is exactly one missing outgoing edge, these faces are represented by quadrilaterals in G_{skel} . We call these quadrilaterals *abstract facial quadrilaterals*.

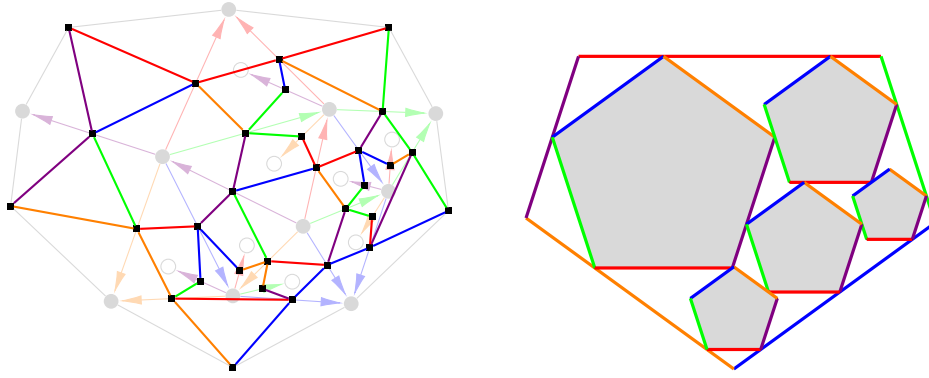


Figure 17: Left: The skeleton graph corresponding to the five color forest in the background. Right: A realization of this skeleton graph as a regular pentagon contact representation.

We color the edges of G_{skel} according to the following rules: If the edge is part of the abstract pentagon of the inner vertex v and lies in the interval between the outgoing edges of v of colors c and $c + 1$, it gets the color $c - 2$. The edges being part of the abstract pentagon of the outer vertex a_i get color i . See Fig. 17 (left) for an example. The colors of the edges of G_{skel} correspond to the required slopes of these edges in the following way: We take a regular pentagon B with horizontal side at the top and color its sides in the colors $1, \dots, 5$ in clockwise order, starting with color 1 at the top side. Then a crossing-free straight line drawing of G_{skel} is a regular pentagon contact representation of G with induced five color forest F if and only if each edge e has the same slope as the side of B that has the same color and all abstract pentagons are regular pentagons, i.e., have five equal side lengths. See Fig. 17 (right).

The purpose of the system of linear equations is to find edge lengths for the edges of G_{skel} . Therefore we have a variable x_v for each inner vertex v of G representing the side length of the corresponding pentagon and a variable for edge of G_{skel} representing its length. The second type of variables can also be defined in the following way: Every inner face f of G gets four variables $x_f^{(1)}, \dots, x_f^{(4)}$ representing the segment lengths of the corresponding quadrilateral in clockwise order where the concave corner is located between the edges corresponding to $x_f^{(1)}$ and $x_f^{(2)}$ (see Fig. 18 (left)). For the five inner faces which are incident to two outer vertices of G we add the equation $x_f^{(1)} = 0$ since these faces are represented by triangles, not by quadrilaterals.

With every inner vertex v we associate five equations, one for each side. Each of these equations states that the side length x_v is equal to the sum of the lengths of the boundary segments of faces incident to the side. More formally, for $i = 1, \dots, 5$, let $\delta_i(v)$ denote the set of faces of G incident to v in the interval between the outgoing edges of colors $i + 2$ and $i - 2$. Then we can write these five equations as $x_v = \sum_{f \in \delta_i(v)} x_f^{(j_{v,f,i})}$ with the $j_{v,f,i} \in \{1, \dots, 4\}$ appropriately chosen. The following lemma gives two more equations for every inner face.

Lemma 28. *Let f be an inner face of G . If the variables $x_f^{(1)}, \dots, x_f^{(4)}$ come from a regular*

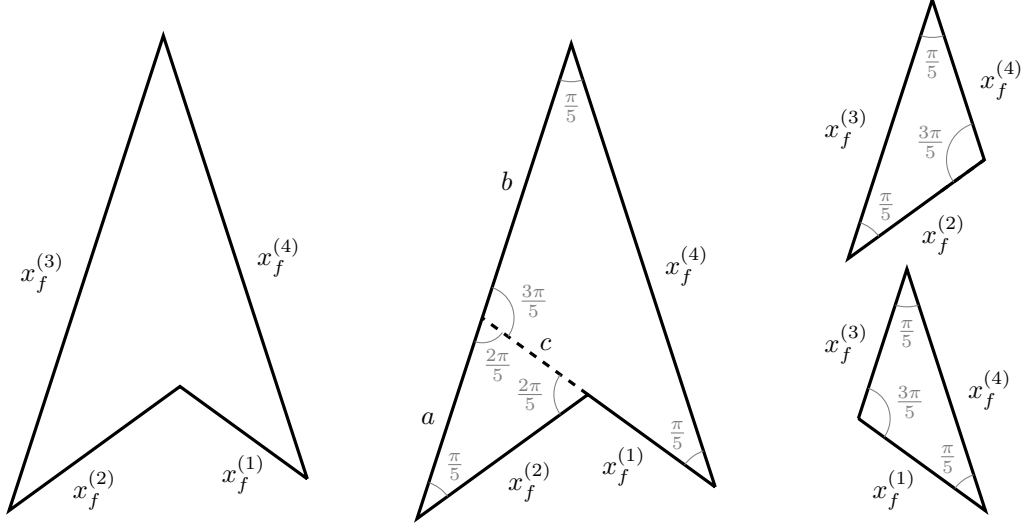


Figure 18: Left: The variables for an inner face f . Middle: The cut as described in the proof of Lemma 28. Right: The two special cases with $x_f^{(1)} = 0$ and $x_f^{(2)} = 0$.

pentagon contact representation of G , they fulfill the following equations:

$$x_f^{(3)} = x_f^{(1)} + \phi x_f^{(2)} \quad , \quad x_f^{(4)} = \phi x_f^{(1)} + x_f^{(2)} \quad .$$

Here $\phi = \frac{1+\sqrt{5}}{2}$ denotes the golden ratio.

Proof. For geometric reasons the three convex corners of the facial quadrilateral corresponding to f are exactly $\frac{\pi}{5}$. Now we cut the quadrilateral along an extension of the edge corresponding to $x_f^{(1)}$ into two triangles. We denote the length of the cut by c . The edge corresponding to $x_f^{(3)}$ is cut into two parts. We denote the lengths of these parts by a and b in clockwise order (see Fig. 18 (middle)). The two resulting triangles have constant inner angles. Thus there are constants $\alpha, \beta, \gamma \in \mathbb{R}$ such that

$$c = \gamma x_f^{(2)} \quad , \quad b = \beta x_f^{(2)} \quad , \quad a = \alpha(x_f^{(1)} + c) \quad .$$

Hence, we have $x_f^{(3)} = a + b = \alpha x_f^{(1)} + (\alpha\gamma + \beta)x_f^{(2)}$. To figure out the constants α and $\alpha\gamma + \beta$ let us consider the special cases that $x_f^{(1)} = 0$ or $x_f^{(2)} = 0$ (see Fig. 18 (right)). In the first case we have $x_f^{(3)} = 2 \cos(\pi/5)x_f^{(2)} = \phi x_f^{(2)}$, in the second case $x_f^{(3)} = x_f^{(1)}$ since the corresponding edges are the legs of an isosceles triangle. Therefore we have $x_f^{(3)} = x_f^{(1)} + \phi x_f^{(2)}$. The second equation can be obtained symmetrically. \square

Finally, we add one more equation to the system which implies that the sum of the lengths of the face edges building the line segment corresponding to the outer vertex a_1 of G is exactly 1, i.e., $\sum_{f \in \delta_1(a_1)} x_f^{(j_{a_1, f, 1})} = 1$ with $j_{a_1, f, 1} \in \{1, \dots, 4\}$ appropriately chosen. See Fig. 19 for an illustration of the different types of equations.

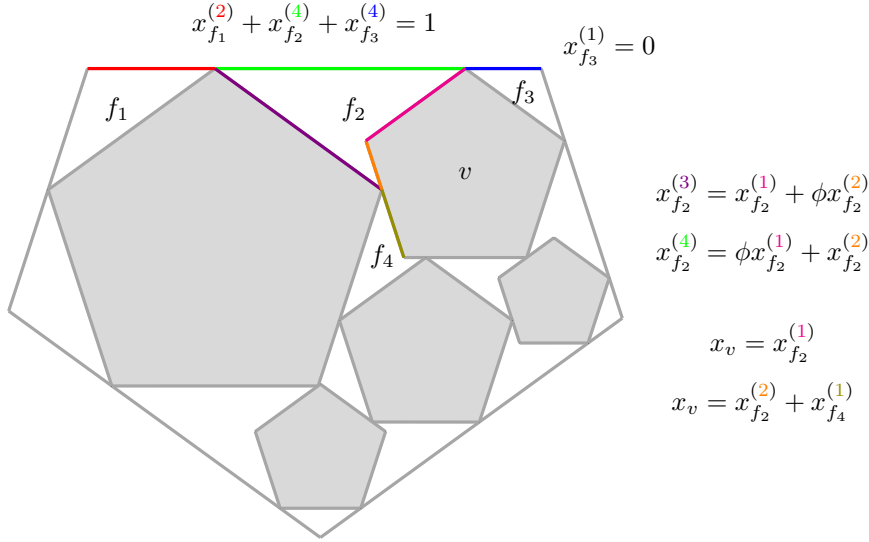


Figure 19: Examples for the different types of equations before substituting the variables $x_{f_i}^{(3)}$ and $x_{f_i}^{(4)}$.

In the equations

$$\sum_{f \in \delta_1(a_1)} x_f^{(j_{a_1, f, 1})} = 1 \quad \text{and} \quad \sum_{f \in \delta_i(v)} x_f^{(j_{v, f, i})} - x_v = 0 \quad (1)$$

we eliminate the variables $x_f^{(3)}, x_f^{(4)}$ using substitutions according to the equations of Lemma 28. The resulting system of linear equations is denoted $A_F \mathbf{x} = \mathbf{e}_1$, here A_F is the coefficient matrix depending on the five color forest F and \mathbf{e}_1 is the first standard unit vector.

We next show that the system of linear equations is uniquely solvable. For this purpose we need a lemma about perfect matchings in plane bipartite graphs. The lemma is well known from the context of Pfaffian orientations, see e.g., [20], we include a proof for completeness. Let H be a bipartite graph with vertex classes $\{v_1, \dots, v_k\}$ and $\{w_1, \dots, w_k\}$. Then a perfect matching of H induces a permutation $\sigma \in \mathcal{S}_k$ by $\sigma(i) = j : \Leftrightarrow \{v_i, w_j\} \in M$. We define the *sign* of a perfect matching M , denoted by $\text{sgn}(M)$, as the sign of the corresponding permutation.

Lemma 29. *Let H be a bipartite graph and let M, M' be two perfect matchings of H . If the symmetric difference of M and M' is the disjoint union of simple cycles C_1, \dots, C_m such that, for $i = 1, \dots, m$, the length ℓ_i of C_i fulfills $\ell_i \equiv 2 \pmod{4}$, then $\text{sgn}(M) = \text{sgn}(M')$.*

If H is a plane graph such that each inner face f of H is bounded by a simple cycle of length $\ell_f \equiv 2 \pmod{4}$, this property is fulfilled for any two perfect matchings of H . Therefore we have $\text{sgn}(M) = \text{sgn}(M')$ for any two perfect matchings M, M' of H in this case.

Proof. For $i = 1, \dots, m$, there is an $n_i \in \mathbb{N}$ with $\ell_i = 4n_i + 2$. Then on the vertices of C_i the permutation σ corresponding to M and the permutation σ' corresponding to M' differ

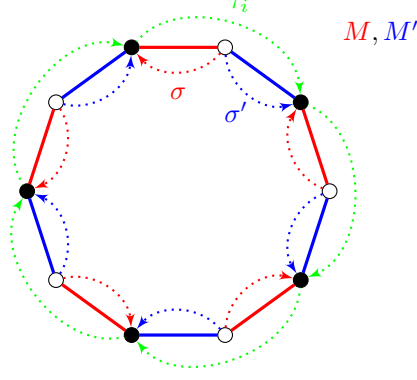


Figure 20: Illustration of $\sigma' = \sigma \circ \tau_i$ in the proof of Lemma 29.

in a cyclic permutation τ_i of length $2n_i + 1$. See Fig. 20. Hence, we have $\sigma' = \sigma \circ \tau_1 \circ \dots \circ \tau_m$ and therefore

$$\begin{aligned} \text{sgn}(\sigma') &= \text{sgn}(\sigma) \cdot \text{sgn}(\tau_1) \cdots \text{sgn}(\tau_m) \\ &= \text{sgn}(\sigma) \cdot (-1)^{2n_1} \cdots (-1)^{2n_m} = \text{sgn}(\sigma) . \end{aligned}$$

In the case that H is a plane graph such that each inner face f of H is bounded by a simple cycle of length $\ell_f \equiv 2 \pmod{4}$, for each cycle of length ℓ with k' vertices in its interior the formula $\ell + 2k' \equiv 2 \pmod{4}$ is valid. This can be shown by induction on the number of faces enclosed by the cycle. Since each of the cycles C_1, \dots, C_m contains an even number of vertices in its interior, this implies $\ell_i \equiv 2 \pmod{4}$ for $i = 1, \dots, m$. \square

Theorem 30. *The system $A_F \mathbf{x} = \mathbf{e}_1$ is uniquely solvable.*

Proof. We show that $\det(A_F) \neq 0$. Let \hat{A}_F be the matrix obtained from A_F by multiplying all columns corresponding to inner vertices of G with -1 . Since in A_F all entries in these columns are non-positive (all vertex-variables have negative coefficients in (1)) and the entries in all other columns are non-negative, all entries of \hat{A}_F are non-negative. Further we have $\det(A_F) = (-1)^n \det(\hat{A}_F)$ where n is the number of inner vertices of G .

Now we want to interpret the Leibniz formula of $\det(\hat{A}_F)$ as the sum over the perfect matchings of a plane auxiliary graph H_F . Let H_F be the bipartite graph whose first vertex class v_1, \dots, v_k consists of the variables of the equation system and whose second vertex class w_1, \dots, w_k consists of the equations of the equation system. There is an edge $v_i w_j$ in H_F if and only if $(\hat{A}_F)_{ij} > 0$. Then we have

$$\det(\hat{A}_F) = \sum_{\sigma} \text{sgn}(\sigma) \prod_i (\hat{A}_F)_{i\sigma(i)} = \sum_M \text{sgn}(M) P_M ,$$

where the second sum goes over all perfect matchings of H_F . The idea of the second equality is to ignore all permutations σ with $\prod_i (\hat{A}_F)_{i\sigma(i)} = 0$ and we have for each perfect matching $M = \{v_1 w_{\sigma(1)}, \dots, v_k w_{\sigma(k)}\}$ a product $P_M = \prod_i (\hat{A}_F)_{i\sigma(i)} > 0$ in the final sum.

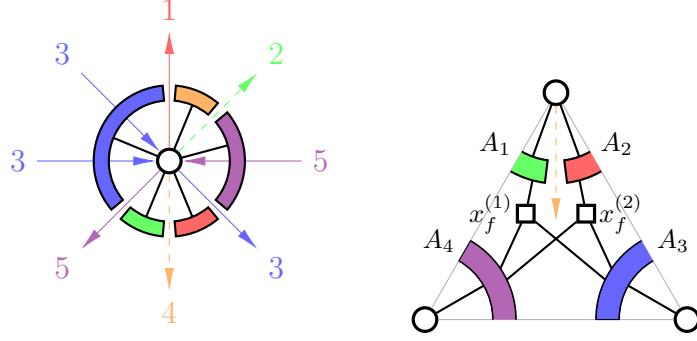


Figure 21: Embedding of H_F into the plane.

Next we will define an embedding of H_F into the plane. See Fig. 21 for an illustration. We start with a crossing-free straight-line drawing of G . Then we draw the missing outgoing edges (see Lemma 9) as segments starting at a vertex and ending inside a face of the drawing. After that we put pairwise disjoint disks around the inner vertices and cut the bordering circles at the intersections with the five outgoing edges of the vertex (including the edges we added in the last step) into five arcs. These five arcs are the drawings of the five equation-vertices incident to the respective vertex and each of these arcs is contained in exactly those faces of the embedding of G which are involved in the corresponding equation. Then every inner face f of G is intersected by exactly four of these arcs, two from the incident vertices with the missing outgoing edge and one from the other two vertices. We denote them by A_1, \dots, A_4 in clockwise order where A_1 and A_2 come from the same vertex. We place the vertices corresponding to $x_f^{(1)}$ and $x_f^{(2)}$ inside f , but outside of the disks of the three incident vertices of f . We connect $x_f^{(1)}$ to A_1 and A_4 , and $x_f^{(2)}$ to A_2 and A_3 . Up to this point the drawing is crossing-free. Finally we add the two intersecting edges $x_f^{(1)}A_3$ and $x_f^{(2)}A_4$ inside f .

Claim 1. *The graph H_F has a perfect matching.*

Proof. We describe an explicit construction of a perfect matching of H_F . The five equation-vertices adjacent to a vertex v of G are corresponding to the five colors of the five color forest. We always match the vertex v with the equation-vertex of color 4. The equation-vertices of colors 2 and 3 are matched with one of the two variable-vertices of the last incident face in clockwise order, and the equation-vertices of colors 5 and 1 are matched with one of the two variable-vertices of the last incident face in counterclockwise order (see Fig. 22 (left)).

Now we will show that each pair of face vertices (except for the five corner-faces, i.e. the five faces incident to two outer vertices) is matched exactly twice. We call a segment of a facial quadrilateral B a *short segment* if it is incident to the concave corner, and we call it a *long segment* otherwise. For two adjacent segments of B we call the segment, whose containing pentagon side ends in the contact point of the two segments, the *cut segment*. Above we mentioned that the five equation-vertices of a vertex of G correspond

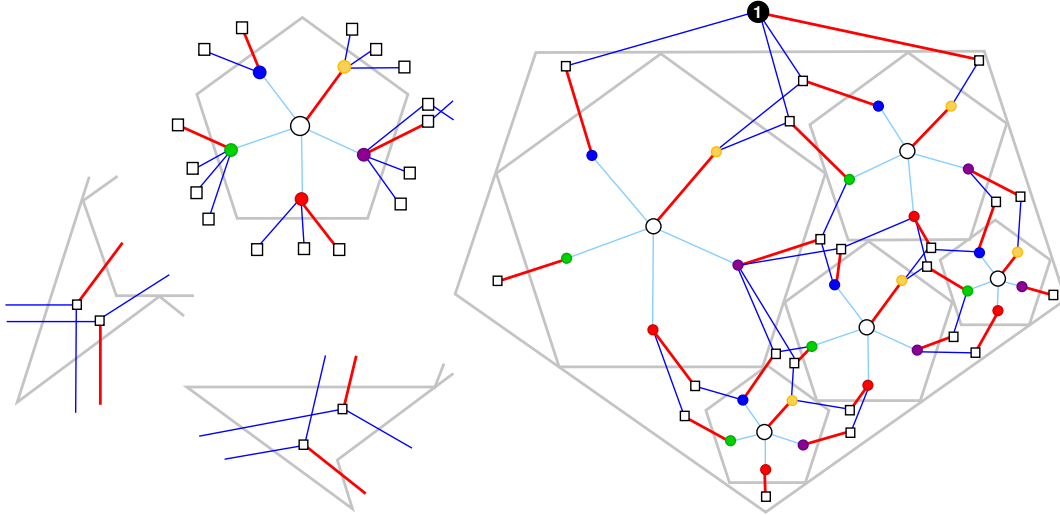


Figure 22: Left: Cases for the construction of the perfect matching. Right: The complete perfect matching in a small instance.

to the five colors. Since each segment of B is involved in exactly one of these equations, we can also associate a color with each of the segments of B . We distinguish three cases concerning segments of color 4 (Fig. 22 (left) shows two of the cases). If B has a short segment of color 4, the other short segment and the cut long segment are matched. If B has a long segment of color 4, the short segment, which is neighboring the segment of color 4, and the cut segment of the two remaining segments are matched. If B has no segment of color 4, for each pair of neighboring long and short segments the cut segment is matched. Hence, in every case the face is matched exactly twice.

Since each face is matched exactly twice, its two variable-vertices are matched exactly once. It can easily be seen that each corner-face is matched exactly once, except the corner-face of color 4 which is not matched. Finally we match the corner-face of color 4 with the equation-vertex corresponding to the non-homogeneous equation, and obtain a perfect matching. Figure 22 (right) shows an example. \triangle

Let \mathcal{M}_0 be the set of perfect matchings of H_F that do not contain both edges of any pair of crossing edges.

Claim 2. *Let $M_1, M_2 \in \mathcal{M}_0$. Then $\text{sgn}(M_1) = \text{sgn}(M_2)$.*

Proof. Since each vertex has degree 1 in M_1 and in M_2 , each vertex has degree 0 or 2 in the symmetric difference of M_1 and M_2 . Therefore the symmetric difference of M_1 and M_2 is a disjoint union of simple cycles. Let C be one of these cycles. Due to Lemma 29 it suffices to show that $\ell(C) \equiv 2 \pmod{4}$.

Now consider a pair $v_a w_b, v_c w_d$ of crossing edges that are both contained in C , i.e., v_a and v_c are the two variable vertices of a face and w_b, w_d correspond to the equations for sidelength of different pentagons, in particular $v_a w_b v_c w_d$ is a 4-cycle in H_F . Since

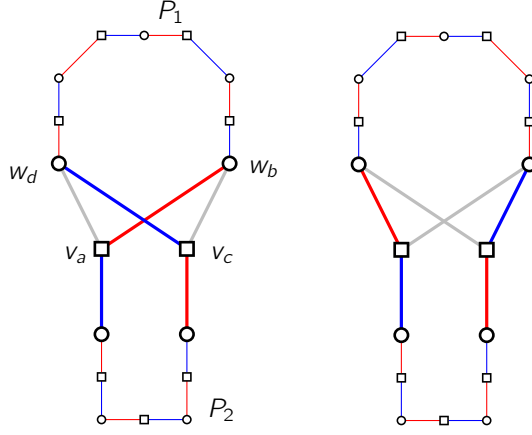


Figure 23: Reducing the number of crossings in the symmetric difference of two perfect matchings of H_F .

the edges $v_a w_b, v_c w_d$ cannot be contained in the same matching, we can assume that the edge $v_a w_b$ is contained in M_1 and the edge $v_c w_d$ in M_2 .

There are two paths P_1, P_2 such that $C = v_a w_b P_1 w_d v_c P_2$. If C looked like $C = v_a w_b P_1 v_c w_d P_2$, the path P_1 would start with an edge of M_2 and end with an edge of M_1 . Therefore P_1 would have even length and the cycle $v_c w_b P_1$ would have odd length, and that is not possible since H_F is bipartite.

Let C' be the cycle defined by $C' := v_c w_b P_1 w_d v_a \overline{P_2}$ where $\overline{P_2}$ denotes the reversed path P_2 . Note that $\ell(C') = \ell(C)$ and that C' is contained in the symmetric difference of the perfect matchings M'_1 and M'_2 obtained from M_1 and M_2 in the following way: In M_1 we replace $v_a w_b$ by $v_a w_d$ and in M_2 we replace $v_c w_d$ by $v_c w_b$. Further all edges of P_1 switch the matching. See Fig. 23.

The swap does not create new crossings since the only new edges $v_a w_d$ and $v_c w_b$ have no crossing edges. Therefore the cycle C' has one crossing less than C . By iterating this process we obtain a cycle C'' with $\ell(C'') = \ell(C)$ which is crossing-free and contained in the symmetric difference of two perfect matchings of H_F . Since C'' is crossing-free, it is also contained in a spanning subgraph H'_F of H_F that keeps all non-crossing edges of H_F and exactly one of the two edges of every crossing pair. Then H'_F inherits a crossing-free drawing from H_F where every inner face is a simple cycle of length 6 (note that every face corresponds to a corner of a pentagon in the pentagon contact representation). Due to Lemma 29 this implies $\ell(C'') \equiv 2 \pmod{4}$. \triangle

Now we will consider all perfect matchings of H_F . We divide them into equivalence classes according to the following equivalence relation: Two perfect matchings M, M' are equivalent if M' can be obtained from M by exchanging pairs of crossing edges with the two non-crossing edges on the same four vertices (we call them *twin edges*). Exchanges in both directions are allowed. Note that each equivalence class contains exactly one of the matchings of \mathcal{M}_0 we considered in Claim 2. Let $M_0 \in \mathcal{M}_0$ be one of these matchings and let $k = k(M_0)$ be the number of pairs of twin edges contained in M_0 . Because each pair

of twin edges can be exchanged independently with the corresponding pair of crossing edges, the equivalence class \mathcal{A}_{M_0} of M_0 consists of 2^k matchings and for $i = 0, \dots, k$, the class contains $\binom{k}{i}$ matchings with exactly i pairs of crossing edges. Note that the entries of A_F corresponding to twin edges are ϕ and that the entries corresponding to crossing edges are 1, see the equations in Lemma 28. Thus in the product P_{M_0} of entries of A_F corresponding to the edges of M_0 we see a contribution of ϕ^2 for each pair of twin edges. The contribution for a pair of crossing edges is 1. Therefore

$$\sum_{M \in \mathcal{A}_{M_0}} \text{sgn}(M) P_M = \sum_{i=0}^k \binom{k}{i} \text{sgn}(M_0) (-1)^i P_{M_0} \left(\frac{1}{\phi^2} \right)^i = \text{sgn}(M_0) P_{M_0} \left(1 - \frac{1}{\phi^2} \right)^k$$

and

$$\det(\hat{A}_F) = \sum_{M_0 \in \mathcal{M}_0} \sum_{M \in \mathcal{A}_{M_0}} \text{sgn}(M) P_M = \sum_{M_0 \in \mathcal{M}_0} \text{sgn}(M_0) \underbrace{P_{M_0}}_{>0} \underbrace{\left(1 - \frac{1}{\phi^2} \right)^{k(M_0)}}_{>0}.$$

Because of Claim 2 we have $\text{sgn}(M_0) = \text{sgn}(M'_0)$ for any two matchings $M_0, M'_0 \in \mathcal{M}_0$. Finally this implies $\det(\hat{A}_F) \neq 0$. \square

The following lemma will help us to prove that a non-negative solution of the system $A_F \mathbf{x} = \mathbf{e}_1$ leads to a regular pentagon contact representation of G .

Lemma 31. *Let H be an inner triangulation of a polygon. For every inner face f of H with vertices v_1, v_2, v_3 in clockwise order let T_f be a triangle in the plane whose vertices have coordinates denoted by $p(f, v_1), p(f, v_2), p(f, v_3)$ in clockwise order such that the following conditions are satisfied:*

(i) *For each inner vertex v of H with incident faces f_1, \dots, f_k*

$$\sum_{i=1}^k \beta(f_i, v) = 2\pi$$

where $\beta(f, v)$ denotes the inner angle of T_f at $p(f, v)$.

(ii) *For each outer vertex v of H with incident faces f_1, \dots, f_k*

$$\sum_{i=1}^k \beta(f_i, v) \leq \pi.$$

(iii) *For each inner edge vw of H with incident faces f_1, f_2*

$$p(f_1, v) - p(f_1, w) = p(f_2, v) - p(f_2, w),$$

i.e., the vector between v and w is the same in T_{f_1} and T_{f_2} .

Then there exists a crossing-free straight line drawing of H such that the drawing of every inner face f can be obtained from T_f by translation.

Proof. Let H^* be the dual graph of H without the vertex corresponding to the outer face of H . Further let S be a spanning tree of H^* . Then by property (iii) we can glue the triangles T_f of all inner faces f of H together along the edges of S . This determines a unique position for every polygon, up to a global motion. We need to show that the resulting shape has no holes or overlappings. For the edges of S we already know that the triangles of the two incident faces are touching in the right way. For the edges of the complement \bar{S} of S we still need to show this. We consider \bar{S} as a subset of the edges of H . Note that \bar{S} is a forest in H . Let e be an edge of \bar{S} incident to a leaf v of this forest that is an inner vertex of H . Then for all incident edges $e' \neq e$ of v we already know that the triangles of the two incident faces of e are touching in the right way. But then also the two triangles of the two incident faces of e are touching in the right way because v fulfills property (i). Since the set of edges we still need to check is still a forest, we can iterate this process until all inner edges of H are checked.

We have to exclude that the resulting polygon has overlappings. Let F be the set of faces of H , let F_{in} be the set of inner faces of G , let V be the set of vertices of H , and let V_{out} be the set of the outer vertices of H . Let $d = |V_o|$.

Claim 1. $\sum_{v \in V_o} \sum_i \beta(f_i, v) = (d - 2)\pi$.

Proof. The sum of the inner angles of each triangle T_f is π . Summing this over all triangles T_f we obtain

$$\sum_{f \in F_{\text{in}}} \pi = (|F| - 1)\pi .$$

Using property (i) we also have

$$\sum_{f \in F_{\text{in}}} \pi = (|V| - d)2\pi + \sum_{v \in V_o} \sum_i \beta(f_i, v) .$$

Using Euler's formula this yields the claim. △

Due to Claim 1 the sum of the angles at the outer vertices is just the right value for a simple d -gon. Because of property (ii) the angles at the boundary are convex. Thus the resulting shape is a simple convex polygon and therefore non-intersecting □

Theorem 32. *The unique solution of the system $A_F \mathbf{x} = \mathbf{e}_1$ is non-negative if and only if the five color forest F is induced by a regular pentagon contact representation of G .*

Proof. Assume there is a regular pentagon representation \mathcal{S} of G that induces the five color forest F . Then the edge lengths given by \mathcal{S} define a non-negative solution of $A_F \mathbf{x} = \mathbf{e}_1$.

For the opposite direction, assume the solution of $A_F \mathbf{x} = \mathbf{e}_1$ is non-negative. To be able to apply Lemma 31 we first construct an internally triangulated extension of the skeleton graph of a hypothetical regular pentagon contact representation with induced five color forest F . We start with a crossing-free straight-line drawing of G . Add a

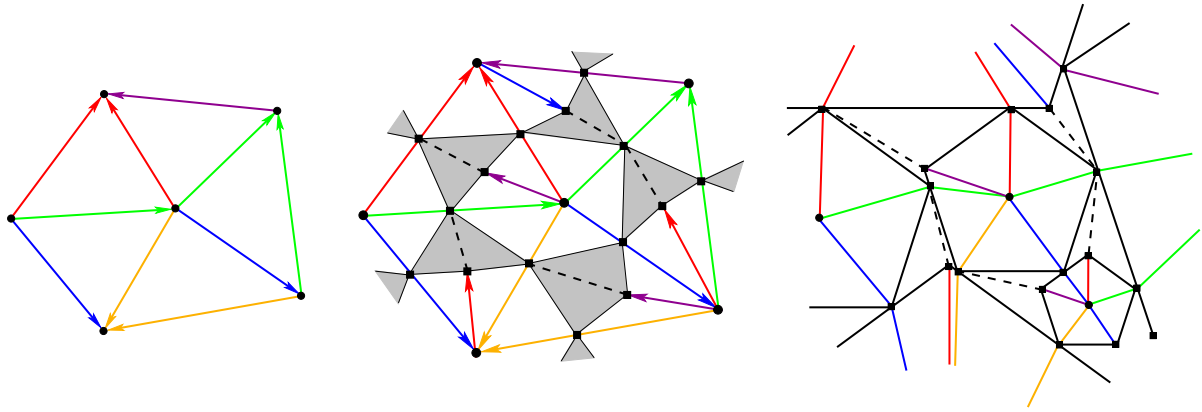


Figure 24: Part of a triangulation with a five color forest, the resulting skeleton graph, and a realization.

subdivision vertex on each edge of G . Moreover, for each inner vertex v draw an edge ending at a new vertex inside each face with a missing outgoing edge of v . Then connect all the new adjacent vertices of v in the cyclic order given by the drawing.

At this point inner faces of G are subdivided into four triangles and a quadrangle (shown gray in Fig. 24). One of the vertices of the quadrangle is the new inner vertex w of the face. Connect vertex w to the subdivision vertex diagonally in the quadrangle (shown dashed in Fig. 24).

Using the edge lengths given by the solution of $A_F \mathbf{x} = \mathbf{e}_1$ we can compute the side length of each triangle T_f corresponding to an inner face f of this skeleton graph such that an application of Lemma 31 gives us a regular pentagon contact representation of G with induced five color forest F . \square

The algorithm first computes an arbitrary five color forest of G (this is possible in linear time by the construction from Theorem 7 since Schnyder woods can be constructed in linear time, see for example [2, 10]). Based on the five color forest the algorithm generates the corresponding system of linear equations and solves it. Since the size of the system is linear in the size of the input graph, this can be done in cubic time, for example with Gaussian elimination. If the solution is non-negative, we can construct the regular pentagon contact representation from the edge lengths given by the solution and we are done. If the solution has negative variables, we would like to change the five color forest and proceed with the new one.

We now show a way of changing the five color forest in the case of a solution with negative variables.

Theorem 33. *The negative and non-negative variables of the solution of $A_F \mathbf{x} = \mathbf{e}_1$ are separated by a disjoint union of directed simple cycles in the α_5 -orientation corresponding to F . If there are negative variables, this union is non-empty.*

Proof. We say that an abstract pentagon or an abstract facial quadrilateral has a *sign-change* at a point p on its boundary if one of the two variables corresponding to the two

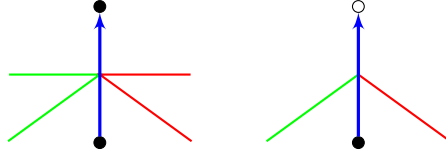


Figure 25: The two types of sign-separating edges. Red (green) edges are edges of the skeleton graph with negative (non-negative) solution values.

boundary edges with common end point p has a negative solution value and the other variable has a non-negative solution value. We call the following two types of edges in the α_5 -orientation *sign-separating edges* (see Fig. 25 for an illustration): Edges of the first type are normal edges vw such that the abstract pentagon of v has a sign-change at the contact point with the abstract pentagon of w , and both abstract facial quadrilaterals incident to this touching point do not have a sign-change at this point. Edges of the second type are stack edges vw with normal vertex v and stack vertex w such that the abstract pentagon of v has a sign-change at the corner which is a concave corner of the abstract quadrilateral of w . Note that both types of sign-separating edges correspond to a corner p of the abstract pentagon A of v fulfilling the following property: One of the two sides of A incident to p starts with a non-negative segment at p and the other side of A incident to p starts with a negative segment at p .

Claim 1. *In an abstract facial quadrilateral there is either no sign-change, or there are two sign-changes (one at a convex corner and one at the concave corner).*

Proof. Let $x_f^{(1)}, \dots, x_f^{(4)}$ be the four variables of the facial quadrilateral as in the beginning of this section (see Fig. 18 (left)). Then the equation system contains the two equations

$$x_f^{(3)} = x_f^{(1)} + \phi x_f^{(2)} \quad , \quad x_f^{(4)} = \phi x_f^{(1)} + x_f^{(2)}$$

where ϕ is the golden ratio. The fact that $\phi > 1$ immediately implies the claim. \triangle

Claim 34. *If there are negative variables, there exists a sign-separating edge.*

Proof. Because of the inhomogeneous equation the solution always contains positive variables. Therefore, if there are negative variables, at some point of the abstract pentagon contact representation there has to be a sign-change.

We distinguish two cases concerning the two possibilities of Claim 1. In the first case there is no sign-change in any abstract facial quadrilateral. Then we can distinguish negative faces (the faces with all four variables negative) and non-negative faces (the faces with all four variables non-negative). The above observation implies that there is at least one face of each kind if there are negative variables. Since the abstract pentagon contact representation is connected, there has to be a point where the abstract facial quadrilaterals of a negative and a non-negative face touch. At such a point there is a sign-separating edge of the first type.

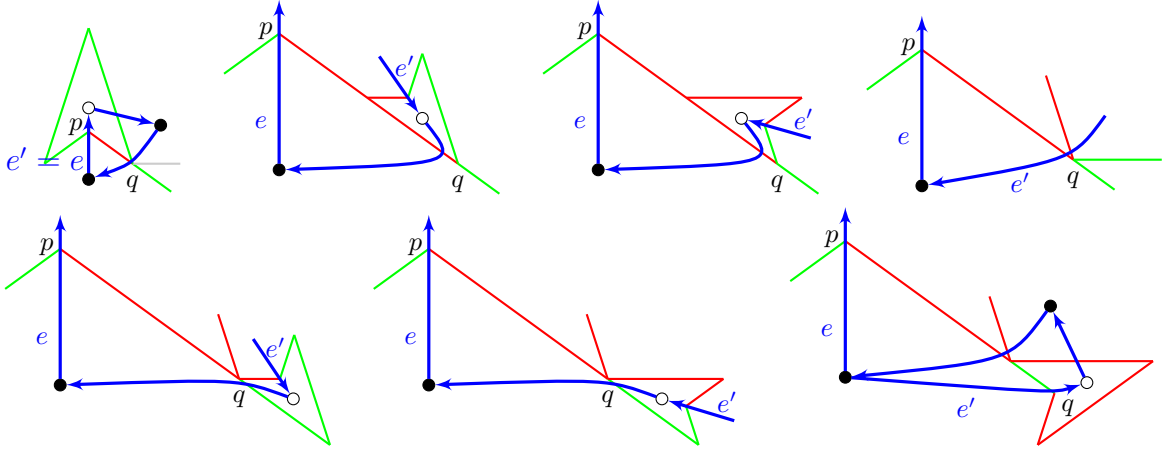


Figure 26: Construction of the predecessors of a sign-separating edge $e = vw$. The last edge e' assigned as a predecessor is a sign-separating edge itself. Therefore the walk can be continued from there by iterating this construction. Red (green) edges are edges of the skeleton graph with negative (non-negative) solution values.

In the second case there exists at least one abstract facial quadrilateral with a sign-change. Due to Claim 1 this abstract facial quadrilateral has a sign-change at its concave corner. Therefore there is a sign-separating edge of the second type. \triangle

For a sign-separating edge $e = vw$ we will now construct an oriented walk in the α_5 -orientation ending in e . Assume that $x_v \geq 0$ (the other case is symmetric). As we noted above, the edge e corresponds to a corner p of the abstract pentagon A of v such that one of the two sides of A incident to p starts with a negative segment at p . If all segments of this side would be negative, this would contradict $x_v \geq 0$. Therefore, when we walk along this side starting at p , there has to be a first point q which is incident to a negative and a non-negative segment. In Fig. 26 we distinguish all possible cases concerning what the abstract pentagon contact representation locally looks like at q (including the signs of the segments) and define the previous one, two or three edges of the walk according to this case distinction. If several edges are added, only the last one is a sign-separating edge itself. Since the last added edge is always a sign-separating edge, the walk can be continued from there by iterating this process.

Let E' be the set of all edges occurring in any predecessor path, including the sign-separating edges. Then we can interpret the predecessor assignment as an assignment from E' to the same set E' .

Claim 2. *The predecessor assignment is a permutation of the set E' .*

Proof. We show that the assignment is injective by proving that each edge e of the α_5 -orientation has a unique successor if it has one. Since E' is a finite set, this implies that the assignment is bijective.

Let $e = vw$ be an edge ending in a stack vertex w . Then e corresponds to the concave corner of the abstract quadrilateral B of w . Let p be the convex corner of B with a sign-

change (this corner is unique due to Claim 1), let A_1 be the abstract pentagon touching p with the interior of a side, and let A_2 be the abstract pentagon touching p with a corner. Further, for $i = 1, 2$, let u_i be the normal vertex corresponding to A_i . If $u_1 = v$, we are in the first or the last case of Fig. 26 and the successor of e has to be the edge wu_2 . Otherwise the successor of e has to be the edge wu_1 .

Now let $e = vw$ be an edge ending in a normal vertex w . If $e \in E'$, it corresponds to a sign-change at a point p in the interior of a side of the abstract pentagon A of w . Let $x_w \geq 0$ (the other case is symmetric). Then the successor of e has to be the edge corresponding to the first corner of A that we reach when we go from p in the direction of the negative segment. \triangle

Due to Claim 2 the edge set E' is a disjoint union of directed simple cycles in the α_5 -orientation separating the negative and non-negative variables. Due to Claim 34 this union is non-empty if there are negative variables. \square

With this theorem at hand we have a way of changing the five color forest and restart the algorithm. We cannot prove that the iteration will eventually stop with a non-negative solution. The following theorem, however, shows in a very special case that the change of the five color forest can have the intended effect, i.e., change the signs of negative variables to positive.

Let g be an oriented cycle in an α_5 -orientation. Then exactly one vertex w of g is a stack vertex. Let s_1 and s_2 be the two edges incident to the concave corner of the abstract facial quadrilateral corresponding to w . Exactly one edge s_i of s_1 and s_2 has an endpoint that is the corner of an abstract pentagon corresponding to a vertex of g . We call s_i the segment *surrounded by g* (see Fig. 16).

Theorem 35. *Let F be a five color forest, let g be an oriented facial cycle in the corresponding α_5 -orientation and let F' be the five color forest obtained from F by flipping g . Let ξ and ξ' be the solutions of the equation systems corresponding to F and F' , respectively. Let s_g be the segment surrounded by g and let ξ_g and ξ'_g be the component of ξ and ξ' , respectively, which corresponds to s_g , i.e., records the 'length' of s_g . Then ξ_g and ξ'_g have different signs or $\xi_g = \xi'_g = 0$.*

Proof. We denote the equation systems corresponding to F and F' as $A_F \mathbf{x} = \mathbf{e}_1$ and $A_{F'} \mathbf{y} = \mathbf{e}_1$. Let f be the face of G containing g . The variable corresponding to s_g in the first system is $x_f^{(i)}$ with $i = 1$ or $i = 2$ and in the second system it is $y_f^{(j)}$ with $j \neq i$ and $j \in \{1, 2\}$, i.e., ξ_g is the value of $x_f^{(i)}$ in the solution ξ and ξ'_g is the value of $y_f^{(j)}$ in the solution ξ' . Let $A_F^{(g)}$ be the matrix obtained from A_F by replacing the column corresponding to $x_f^{(i)}$ with \mathbf{e}_1 , and let $A_{F'}^{(g)}$ be the matrix obtained from $A_{F'}$ by replacing the column corresponding to $y_f^{(j)}$ with \mathbf{e}_1 . According to Cramer's rule we have

$$\xi_g = \frac{\det(A_F^{(g)})}{\det(A_F)}, \quad \xi'_g = \frac{\det(A_{F'}^{(g)})}{\det(A_{F'})}.$$

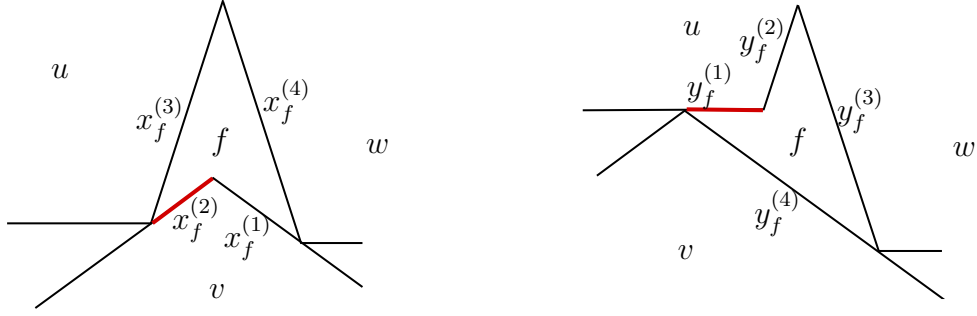


Figure 27: The face f before and after the flip at the red segment together with the variables of the face.

It can be verified that the column of A_F corresponding to $x_f^{(j)}$ and the column of $A_{F'}$ corresponding to $x_f^{(i)}$ are equal. We go through the details with the generic example shown in Fig. 27. In this case $i = 2$ and $j = 1$. Consider the variable $x_f^{(1)}$. It naturally belongs to the equation of color 4 of v with a coefficient of 1. Due to the substitutions, see the equations in Lemma 28, it also contributes to the equations of color 5 at u and of color 2 at w , the respective coefficients are 1 and ϕ . Now consider the variable $y_f^{(2)}$. It naturally belongs to the equation of color 5 of u with a coefficient of 1. The substitutions also make it contribute to the equations of color 4 at v and of color 2 at w , the respective coefficients are 1 and ϕ . Hence, the columns corresponding to $x_f^{(1)}$ and $y_f^{(2)}$ in their respective systems are equal.

If we switch the columns corresponding to $y_f^{(i)}$ and $y_f^{(j)}$ in $A_{F'}$ to get $\tilde{A}_{F'}$, then, by the above A_F and $\tilde{A}_{F'}$ only differ in the column corresponding to the segment s_g , whence $A_F^{(g)} = \tilde{A}_{F'}^{(g)}$.

To prove the theorem it remains to show that $\det(A_F)$ and $\det(\tilde{A}_{F'})$ have different signs. Similar to the proof of Theorem 30 we can do this by showing that a perfect matching M of H_F and a perfect matching M' of $H_{F'}$ that both do not contain a pair of crossing edges, have different signs.

Let v_1 and v_2 be the vertices of H_F and $H_{F'}$ corresponding to face f such that v_1 corresponds to s_g . Note that this makes the local situations around f in H_F and $H_{F'}$ asymmetric (see Fig. 28). The asymmetry corresponds to the switch of columns from $A_{F'}$ to $\tilde{A}_{F'}$.

Let w_1 be the unique equation-vertex that is adjacent to v_1 and v_2 in F and F' (in Fig. 27 vertex w_1 would correspond to the equation of color 2 at w). Let w_2 be the equation-vertex that is adjacent to both of v_1 and v_2 only in F , and in F' only to v_2 (in Fig. 27 vertex w_2 would correspond to the equation of color 5 at u). Let w_3 be the equation-vertex belonging to the same pentagon as w_2 that is adjacent to v_1 in F' (in Fig. 27 vertex w_3 also belongs to u and has color 1). Let w_4 be the equation-vertex that is adjacent to v_1 in F and has no adjacency in F' (in Fig. 27 vertex w_4 corresponds to the equation of color 3 at v). Finally, let w_5 be the equation-vertex belonging to the same pentagon as w_4 that is adjacent to both of v_1 and v_2 in F' , and in F only to v_2 (in Fig. 27

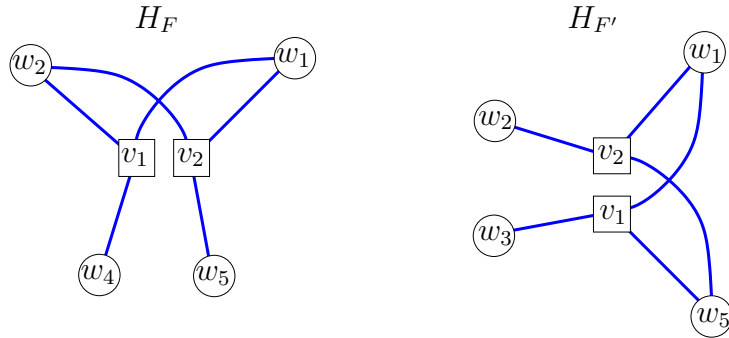


Figure 28: The local situation around f in H_F and $H_{F'}$.

vertex w_5 corresponds to the equation of color 4 at v).

The non-crossing condition implies that M does not contain both of the edges v_1w_1 and v_2w_2 , and that M' does not contain both of the edges v_1w_1 and v_2w_4 .

We distinguish two cases. In the first case, both of M and M' contain the edge v_1w_1 . Then M has to contain the edge v_2w_5 and M' has to contain the edge v_2w_2 . In this case M' is a matching of H_F which contains a single crossing while M is a matching without crossing. Therefore, $\text{sgn}(M) \neq \text{sgn}(M')$.

In the second case, at least one of the matchings M and M' does not contain the edge v_1w_1 . Assume M' contains the edge v_1w_j with $j \in \{3, 4\}$ and not the edge v_1w_1 . The case where M does not contain the edge v_1w_1 is symmetric. Note that we can add the edge v_1w_j to H_F without creating an additional crossing and let \hat{H} be the thus obtained graph. Then M and M' are matchings of \hat{H} . If we delete one edge of each pair of crossing edges from H_F , all inner faces are bounded by simple cycles of length 6. By doing the same with \hat{H} one of the 6-cycles is divided into two cycles of length 4 by the edge v_1w_j .

To argue that $\text{sgn}(M) \neq \text{sgn}(M')$ we define the graph \tilde{H} obtained from \hat{H} by subdividing the edge v_1w_j into three edges v_1u_1, u_1u_2, u_2w_j . Then, if we delete one edge of each pair of crossing edges from \tilde{H} , all inner faces are bounded by simple cycles of length 6. Let \tilde{M} be the perfect matching of \tilde{H} obtained from M by adding the edge u_1u_2 , and let \tilde{M}' be the perfect matching of \tilde{H} obtained from M' by replacing the edge v_1w_j with the edges v_1u_1 and u_2w_j . Then the symmetric difference of \tilde{M} and \tilde{M}' is a disjoint union C_1, \dots, C_k of simple cycles of lengths $\ell(C_i) \equiv 2 \pmod{4}$. Let C_1 be the cycle containing the edges v_1u_1, u_1u_2, u_2w_j . Then the symmetric difference of M and M' is the disjoint union of the cycles C_2, \dots, C_k and the cycle C'_1 obtained from C_1 by replacing the edges v_1u_1, u_1u_2, u_2, w_j with the edge v_1w_j . Therefore $\ell(C'_1) \equiv 0 \pmod{4}$ and $\text{sgn}(M) \neq \text{sgn}(M')$. \square

4 Concluding remarks

We cannot prove that the iterations of the algorithm lead to any kind of progress. Therefore, it may be that the algorithm cycles and runs forever. However, there are two independent implementations [12, 14] of the algorithm and experiments with these imple-

mentations have always been successful.

Similar algorithms for the computation of contact representations with homothetic squares or triangles have been described in [7] and [8]. These algorithms have also been subject to extensive experiments [11, 13] that have always been successful. We therefore have the following conjecture.

Conjecture 36. The algorithm described above terminates with a non-negative solution for every graph G which is an inner triangulation of a 5-gon, and for every initial five color forest F of G .

A proof of this conjecture would imply a new proof for the existence of pentagon contact representations for these graphs. Moreover, since they only depend on the values of the solution of a linear system of equations, the coordinates for the corners of the pentagons could be computed exactly. If the proof would come with a polynomial bound on the number of iterations before termination, then the algorithm would run in strongly polynomial time when doing arithmetics in the extension field $\mathbb{Q}[\sqrt{5}]$ of the rationals.

References

- [1] Olivier Bernardi and Éric Fusy. Schnyder decompositions for regular plane graphs and application to drawing. *Algorithmica*, 62:1159–1197, 2012.
- [2] Enno Brehm. 3-orientations and Schnyder 3-tree-decompositions. Diplomarbeit, Freie Universität Berlin, 2000. URL: page.math.tu-berlin.de/~felsner/Diplomarbeiten/brehm.ps.gz.
- [3] Rowland L. Brooks, Cedric A. B. Smith, Arthur H. Stone, and William T. Tutte. The dissection of rectangles into squares. *Duke Mathematical J.*, 7:312–340, 1940.
- [4] Hubert de Fraysseix and Patrice Ossona de Mendez. On topological aspects of orientations. *Discrete Mathematics*, 229(1):57–72, 2001.
- [5] Hubert de Fraysseix, Patrice Ossona de Mendez, and Pierre Rosenstiehl. On triangle contact graphs. *Combinatorics, Probability and Computing*, 3:233–246, 1994.
- [6] Stefan Felsner. Lattice structures from planar graphs. *Electronic J. of Combinatorics*, 11(1):R15, 2004.
- [7] Stefan Felsner. Triangle contact representations. In *Midsummer Combinatorial Workshop, Praha*, 2009. URL: page.math.tu-berlin.de/~felsner/Paper/prag-report.pdf.
- [8] Stefan Felsner. Rectangle and square representations of planar graphs. In *Thirty Essays on Geometric Graph Theory*, pages 213–248. Springer, 2013.
- [9] Daniel Gonçalves, Benjamin Lévêque, and Alexandre Pinlou. Triangle contact representations and duality. *Discrete and Computational Geometry*, 48(1):239–254, 2012.
- [10] Stephen G. Kobourov. Canonical orders and Schnyder realizers. In *Encyclopedia of Algorithms*, pages 277–283. Springer, 2016.

- [11] Thomas Picchetti. Finding a square dual of a graph. 2011. URL: page.math.tu-berlin.de/~felsner/Diplomarbeiten/rapport_picchetti.pdf.
- [12] Nadine Raasch. Kontaktdarstellungen planarer Graphen mit Fünfecken. Masterarbeit, Technische Universität Berlin, 2018. URL: page.math.tu-berlin.de/~felsner/Diplomarbeiten/Masterarbeit_Nadine-Raasch.pdf.
- [13] Julia Rucker. Kontaktdarstellungen von planaren Graphen. Diplomarbeit, Technische Universität Berlin, 2011. URL: page.math.tu-berlin.de/~felsner/Diplomarbeiten/dipl-Rucker.pdf.
- [14] Manfred Scheucher and Hendrik Schrezenmaier. k -Contact Representations, 2018. URL: <https://www3.math.tu-berlin.de/diskremath/research/kgon-representations/index.html>.
- [15] Walter Schnyder. Embedding planar graphs on the grid. In *Proc. SODA*, pages 138–148, 1990.
- [16] Oded Schramm. Combinatorically prescribed packings and applications to conformal and quasiconformal maps. Modified version of PhD thesis from 1990. [arXiv:0709.0710v1](https://arxiv.org/abs/0710.0710v1).
- [17] Oded Schramm. Square tilings with prescribed combinatorics. *Israel J. of Mathematics*, 84(1-2):97–118, 1993.
- [18] Hendrik Schrezenmaier. Zur Berechnung von Kontaktdarstellungen. Masterarbeit, Technische Universität Berlin, 2016. URL: page.math.tu-berlin.de/~schrezen/Papers/Masterarbeit.pdf.
- [19] Raphael Steiner. Existenz und Konstruktion von Dreieckszerlegungen triangulierter Graphen und Schnyder woods. Bachelorarbeit, FernUniversität in Hagen, 2016. URL: www.fernuni-hagen.de/mathematik/DMO/pubs/Bachelorarbeit_Raphael_Steiner.pdf.
- [20] Robin Thomas. A survey of Pfaffian orientations of graphs. In *International Congress of Mathematicians. Vol. III*, pages 963–984. Eur. Math. Soc., 2006.